SUBSURFACE STUDIES OF FIMKASSAR AREA USING SEISMIC AND WELL DATA

BY

MUHAMMAD USMAN

BS. GEOPHYSICS

(2013-2017)

DEPARTMENT OF EARTH SCIENCES

QUAID-I-AZAM UNIVERSITY

ISLAMABAD

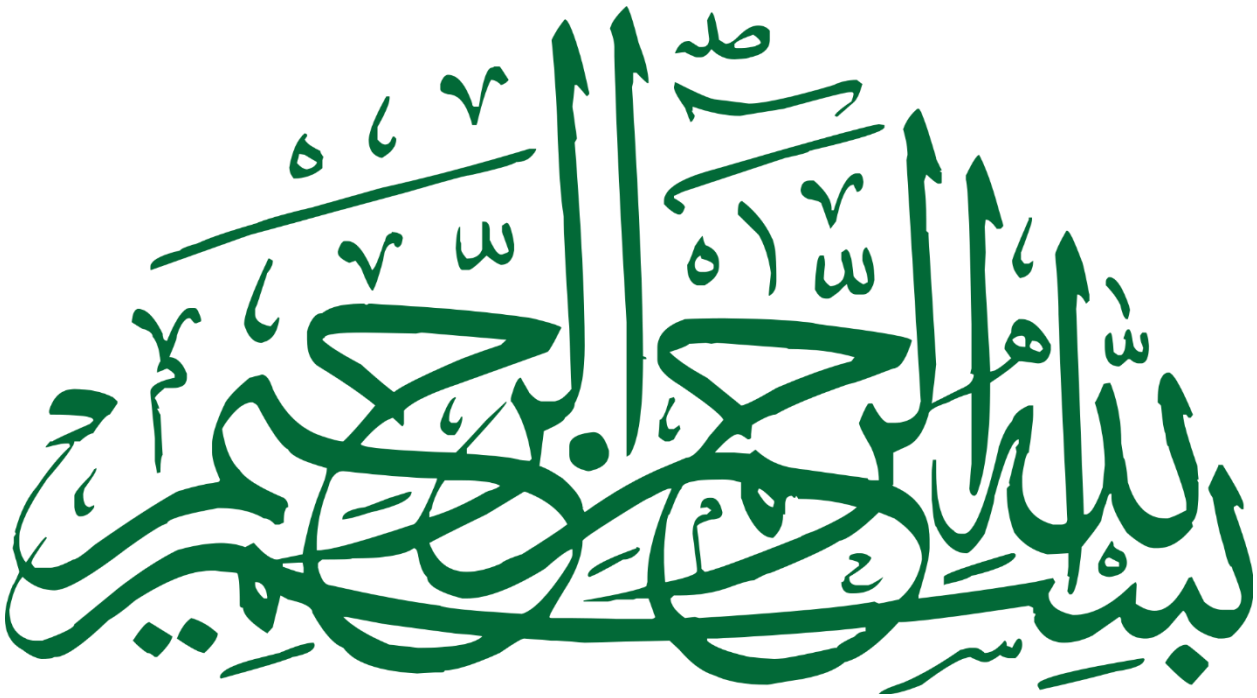

“In the Name of ALLAH, the Most Merciful & Mighty”

“PAY THANKS TO ALLAH EVERY MOMENT AND GO TO EXPLORE THE HIDDEN TREASURES, ITS ALL FOR YOUR BENEFIT”

(AL-QURAN).

CERTIFICATE OF APPROVAL

This dissertation submitted by **MUHAMMAD USMAN** S/O **GULZAR AHMED** is accepted in its present form by the Department of Earth Sciences, Quaid-i-Azam University Islamabad as satisfying the requirement for the award of bachelor of science degree in Geophysics.

Recommended By

DR. AAMIR ALI
(Supervisor) _____

PROF. DR. MONA LISA
(Chairperson Department of Earth Sciences) _____

EXTERNAL EXAMINER _____

ACKNOWLEDGEMENT

First praise is to Allah, the most Beneficent, Merciful and Almighty, on whom ultimately, we depend for sustenance and guidance. I bear witness that Holy Prophet Muhammad (PBUH) is the last messenger, whose life is perfect model for the whole mankind till the Day of Judgment. I thank Allah for giving me strength and ability to complete this study.

Foremost, I would like to express my sincere gratitude to my Supervisor **DR. AAMIR ALI** for the continuous support of my dissertation, for his patience, motivation, enthusiasm, and immense knowledge. His guidance helped me in all the time of research and writing of this dissertation. I also wish to thank the whole faculty and senior students of my department for providing me with an academic base, which has enabled me to take up this study. I pay my thanks to my best friends and employees of clerical office who helped me a lot. Last but not the least I specially acknowledge the prayers and efforts of my whole family, specially my parents for their encouragement, support and sacrifices throughout the study.

MUHAMMAD USMAN

BS. GEOPHYSICS

(2013-2017)

SUMMARY

Reservoir characterization using seismic and Well data is a renowned technique within the context of hydrocarbon exploration. This study pertains to the interpretation of seismic lines, wireline logs and spectral decomposition for better visualization of important features at reservoir level.

The study area selected for this purpose is Fimkassar area (Upper Indus Basin) Pakistan. The area is a part of Potwar sub-basin which is known for its hydrocarbon structural traps. Patala formation acts as a source rock, Chorgali and Sakesar formation acts a reservoir rock whereas Murree formation acts a seal/cap rock.

The data used for this work consist of 3 seismic lines. The result suggest that study area consists of snake head structures and pop-up anticlines.

Various seismic attributes are used to confirm the interpretation results.

Spectral Decomposition further used which helps in identifying bed thicknesses and geologic discontinuities. The result suggests that at 37.3 Hz Sakesar formation produce better results in regard of hydrocarbon exploration. Spectral decomposition results are further verified by petrophysical analysis of Sakesar formation.

Petrophysical analysis of Well Fimkassar-02 is carried out for Chorgali, Sakesar and Patala formation to depict the favorable zones for hydrocarbon accumulation and their reservoir characteristics. The results suggest that Sakesar formation is more producing then Chorgali formation. Average hydrocarbon saturation in Sakesar formation is 55% and average porosity is 5%.

Table of Contents

Chapter# 01 ..... **1**

INTRODUCTION **1**

1.1 Introduction: 2

1.2 Introduction to The Study Area: 2

1.3 Exploration History of Fimkassar Oil Field: 3

1.4 Objectives of Dissertation: 4

1.5 Data Used: 4

1.6 Software Tools Used: 4

1.7 Base Map of Study Area: 5

1.8 Work Flow: 5

Chapter # 02 ..... **6**

GENERAL GEOLOGY, TECTONICS AND STRATIGRAPHRY OF UPPER INDUS BASIN **6**

2.1 Regional Geology: 7

2.2 Tectonic of Potwar Basin: 8

2.2.1 Major Faults in Potwar Basin: 8

2.2.2 Major Folds in Potwar Basin: 9

2.3 Structures in Potwar Region: 9

2.4 Stratigraphy of Eastern Potwar Basin: 9

2.5 Petroleum Play: 10

2.5.1 Source Rock: 10

2.5.2 Reservoir Rock: 10

2.5.3 Seal/Cap/Trap Rock: 10

CHAPTER # 03 ..... **12**

SEISMIC DATA INTERPRETATION **12**

3.1 Introduction: 13

3.2 Structural Interpretation: 13

3.3 Synthetic Seismogram: 15

3.4 Interpretation of Seismic Lines: 16

3.4.1 Identification of Faults: 16

3.4.2 Marking of Seismic Horizon: 16

3.5 Interpreted Seismic Sections: 16

3.6 Fault Polygon Generation: 18
3.7 Contour Maps: 18
3.8 Time and Depth Contour Maps of Chorgali Formation: 19
3.9 Time and Depth Contour Map of Sakeser Formation: 21
3.10 Time and Depth Contour of Patala Formation: 22
3.11 Identification of Well Location: 24
3.11.1 Lead-01: 24
3.12 Seismic Attributes: 26
3.12.1 The Classification of Attributes: 26
3.12.2 Application of Seismic attributes on the seismic line: 27
CHAPTER # 04 30
SPECTRAL DECOMPOSITION 30
4.1 Introduction: 31
4.2 Preamble: 31
4.3 Methodology: 31
4.4 Application of Spectral Decomposition: 32
4.4.1 Identifying Minor Faults: 32
4.4.2 Identifying prospect hydrocarbon zones. 34
4.5 Comparison of Grids at Different Frequency Ranges: 35
4.5.1 Chorgali Grids: 35
4.5.2 Sakesar Grid: 37
CHAPTER# 05 39
PETROPHYSICS 39
5.1 Introduction: 40
5.2 Well Data Used: 40
5.3 Logs Used: 40
5.4 Volume of Shale: 42
5.4.1 Gamma Ray Log: 42
5.4.2 Calculation of Volume of Shale: 42
5.5 Porosity: 42
5.5.1 Calculation of Porosity from Sonic Log: 43
5.5.2 Calculation of Porosity from Density Log: 43
5.5.3 Calculation of Average Porosity: 44

5.5.4 Calculation of Total Porosity: 44
5.5.5 Calculation of Effective Porosity: 44
5.6 Calculation of Water Saturation (**Sw**): 45
5.6.1 Calculation of Resistivity of Water (***Rw***): 45
5.6.2 Calculation of Resistivity of water Equivalent (**Rweq**) and **Rw**: 47
5.7 Well Log Interpretation of Fimkassar-02 48
5.7.1 Petrophysical Interpretation of Chorgali Formation: 48
5.7.2 Petrophysical Interpretation of Sakesar Formation: 50
Conclusions: 53
References: 54

List of Figures:

- Figure 1.1: Satellite image of the Fimkassar area the red block showing the positon of the area.
- Figure 1.2: Base map of the study area
- Figure 1.3: Work flow adopted.
- Figure 2.1: Map Showing study area and geological boundaries (Banks and Warburton, 1986).
- Figure 2.2: Geological and structural map of Potwar (Khan, 1986; Gee, 1989).
- Figure 2.3: Schematic stratigraphic column of eastern Potwar (Aamir and Siddiqui, 2006).
- Figure 3.1: Interpretation Work Flow
- Figure 3.2: Synthtic siesmogram developed at Turkwal-01 well
- Figure 3.3: Interpreted seismic line S96-PW-04.
- Figure 3.4: Interpreted seismic line G884-FMK-106.
- Figure 3.5: Interpreted seismic line S96-PW-02.
- Figure 3.6: Polygon's orientation on base map.
- Figure 3.7: TWT contour map of Chorgali Formation.
- Figure 3.8: Depth contour map of Chorgali Formation.
- Figure 3.9: TWT contour map of Sakesar Formation.
- Figure 3.10: Depth contour map of Sakesar Formation.
- Figure 3.11: TWT contour map of Patala Formation.
- Figure 3.12: Depth contour map of Patala Formation.
- Figure 3.13: Identification of leads of Chorgali Formation.
- Figure 3.14: Identification of leads of Sakesar Formation.
- Figure 3.15: Identification of leads of Patala Formation.
- Figure 3.16: Trace envelop attribute extracted on line S96-PW-04.
- Figure 3.17: Average energy attribute extracted on line S96-PW-04.
- Figure 4.1: Spectral decomposition used to identify thin beds through analysis of the frequency spectrum in a short window around the time of the bed (Partyka et al., 1999).
- Figure 4.2: Different seismic response at different frequencies much more seismic detailed can be ascertained with the 37 Hz iso-frequency data set as compared to 23 Hz (Partyka et al., 1999).
- Figure 4.3: Shows minor fault at dominant frequency of 37.3 Hz.

- Figure 4.4: Comparison with seismic sections transformed by different spectral decomposition method. (a: original seismic trace, b: seismic section at 8 Hz, c: seismic trace at 10 Hz, d: seismic trace at 15.5 Hz).
- Figure 4.5: Work flow adopted for spectral decomposition for this study.
- Figure 4.6: Chorgali grid at 15Hz.
- Figure 4.7: Chorgali grid at 30Hz.
- Figure 4.8: Chorgali grid at 37.3Hz.
- Figure 4.9: Sakesar grid at 15Hz.
- Figure 4.10: Sakesar grid at 30Hz.
- Figure 4.11: Sakesar grid at 37.3Hz.
- Figure 5.1: Petrophysical analysis work flow (Ali et al., 2014).
- Figure 5.2 Determination of Rw from SP chart (Schlumberger, 1989).
- Figure 5.3: Petrophysical interpretation of the well Fimkassar-02 with possible hydrocarbon zone.
- Figure 5.4: Petrophysical interpretation of the well Fimkassar-02 with possible hydrocarbon zone.

List of Tables:

- Table 1.1: Seismic survey lines used for dissertation.
- Table 1.2: Well data details used for dissertation.
- Table 5.1: Logs Used and their Scales.
- Table 5.2: Logs Used in different Tracks.
- Table 5.3: Value of SSP, SP_{clean}, SP_{shale} for the well Fimkassar-02.
- Table 5.4: For whole depth of Chorgali Formation.
- Table 5.5: For interested zone in Chorgali Formation.
- Table 5.6: For whole depth of Sakesar Formation.
- Table 5.7: For interested zone of Sakesar Fomation.

Chapter# 01

INTRODUCTION

1.1 Introduction:

The goal of reservoir characterization is to provide a 2D geological model to petroleum engineers for reservoir performance simulation and for well planning (Slatt, 2006).

In 1915, exploration geophysicists started working on seismic method because of its high resolution and improved accuracy. It became quite useful for imaging subsurface geological features and for identifying structural or stratigraphic traps (Coffeen, 1986). Seismic Reflection Method most commonly used in hydrocarbon exploration in petroleum geology. Petroleum system mainly comprises of three constituents that are enlisted below.

- Source rocks (contains organic materials which for responsible for generation of hydrocarbons).
- Reservoir rocks (migration of hydrocarbons takes place from source rock and reservoir rock offers suitable conditions for their accumulation).
- Seal or trap rocks (act as a barrier it stops upward movement of hydrocarbons).

Petrophysical analysis estimate the physical properties of reservoir such as volume of shale, porosity, water and hydrocarbon saturation which help in identifying the zones of interest (Ali et al., 2014).

Spectral decomposition transforms the seismic data into the frequency domain by using mathematical methods such as discrete Fourier transform, continuous wavelet transforms. The transformed results include tuning cubes and a variety of discrete common frequency cubes. Spectral decomposition has proven to be a robust approach for seismic interpretation. They are used for mapping temporal bed thickness (Partyka et al., 1998, 1999), to indicate stratigraphy traps (Marfurt and Kirlin, 2001), and estimates hydrocarbon zones (Castagna et al., 2003).

1.2 Introduction to The Study Area:

Geographically, Fimkassar area is in Chakwal district of Punjab province. Geologically it is located in eastern part of Potwar Basin, Upper Indus basin, bounded by Soan syncline in the north, Salt Ranges in the south, Jhelum fault in east and Kalabagh fault in west (Siddiqui et al., 1998). The elevation and the coordinates of the study area are given below. Satellite image of Fimkassar area is shown in Figure 1.1.

- **Latitude: 33°4'53"N**
- **Longitude: 72°56'11"E**
- **Elevation: 515 m**

Figure 1.1: Satellite image of the Fimkassar area the red block showing the position of the area.

1.3 Exploration History of Fimkassar Oil Field:

Fimkassar oil and gas field is located about 75 kilometers Southwest (SW) of Islamabad, in the northern Pakistan. The field was discovered in 1980 by Gulf Oil Company (GOC), which drilled a well named, the Fimkassar-1X. 20 barrels of oil per day was produced by this well and the field was declared non-commercial field and was sold to a local company of Pakistan, Oil and Gas Development Corporation Limited (OGDCL). OGDCL drilled a well named, Fimkassar-1A but the well was abandoned due to technical problems. Fimkassar-1-ST was drilled and it was the highest oil volume producer well and it produced about 4,000 barrels/day. In 1990, well named as Fimkassar-2 was drilled. This well initially produced 1960 barrels of oil per day. Fimkassar produces oil and gas from a very stiff limestone that have very low porosity and permeability. Patala (Paleocene) formation is major source of hydrocarbon at Fimkassar field (Khan et al., 1986). The Shales of Murree (Miocene) formation provide a seal for hydrocarbon.

1.4 Objectives of Dissertation:

The main Objectives of dissertation are given below

- Detailed 2D seismic interpretation for identification of the structures favorable for hydrocarbon accumulation.
- Petrophysical analysis for the identification of favorable zones for hydrocarbon accumulation and their reservoir characteristics.
- Spectral Decomposition for better visualization of important features at reservoir level.

1.5 Data Used:

To achieve all the objectives that are listed above following data is provided by the Department of Earth Sciences Quaid-i-Azam University Islamabad and used for completion of this dissertation.

Table 1.1: Seismic survey lines used for dissertation.

Seismic lines	**Nature of Line**
S96-PW-02	Dip
S96-PW-04	Dip
G884-FMK-106	Strike

Table 1.2: Well data details used for dissertation.

Well Name	**Well Depth**	**Formation Top(Sakesar)**	**Discovery**
Turkwal-01	3250	3067	Oil & Gas
Fimkassar-02	3067	2946	Oil & Gas

1.6 Software Tools Used:

To complete the Project and completion of this dissertation following Software and tools are used:

- SMT KINGDOM 8.8.
- SnagIt 13.

1.7 Base Map of Study Area:

Figure 1.2 shows the base map of the study area. Two dip lines (NW-SE) and one strike line (E-W) are used.

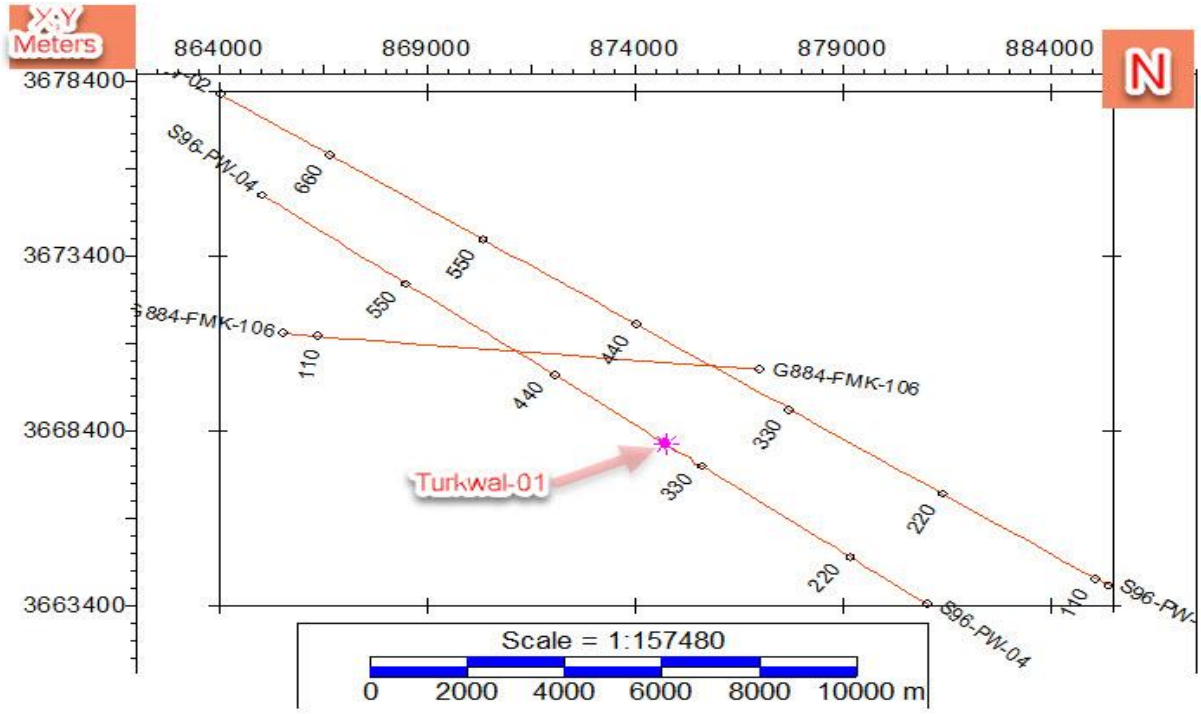

Figure 1.2: Base map of the study area.

1.8 Work Flow:

Figure 1.3 shows the overall work flow adopted in this study.

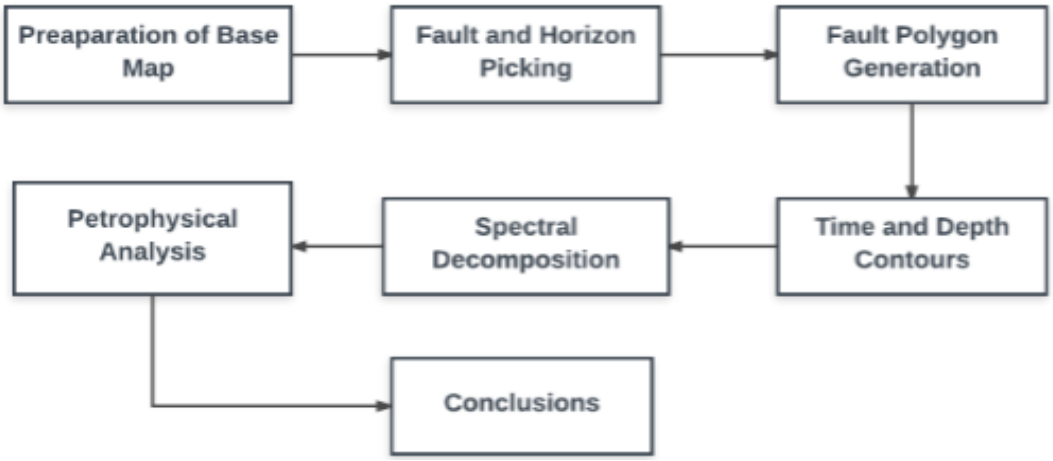

Figure 1.3: Work flow adopted.

Chapter # 02

GENERAL GEOLOGY, TECTONICS AND STRATIGRAPHRY OF UPPER INDUS BASIN

2.1 Regional Geology:

Our study area lies in Potwar plateau which is an elevated and nearly flat region. In the north of Potwar plateau there is Kalachitta and Margalla Hills, Salt Ranges in the south, the Jhelum fault and the Hazara-Kashmir Syntaxes to the east and Kalabagh fault in west (Kazmi & Jan, 1997). The study area marked by block is shown in Figure 2.1.

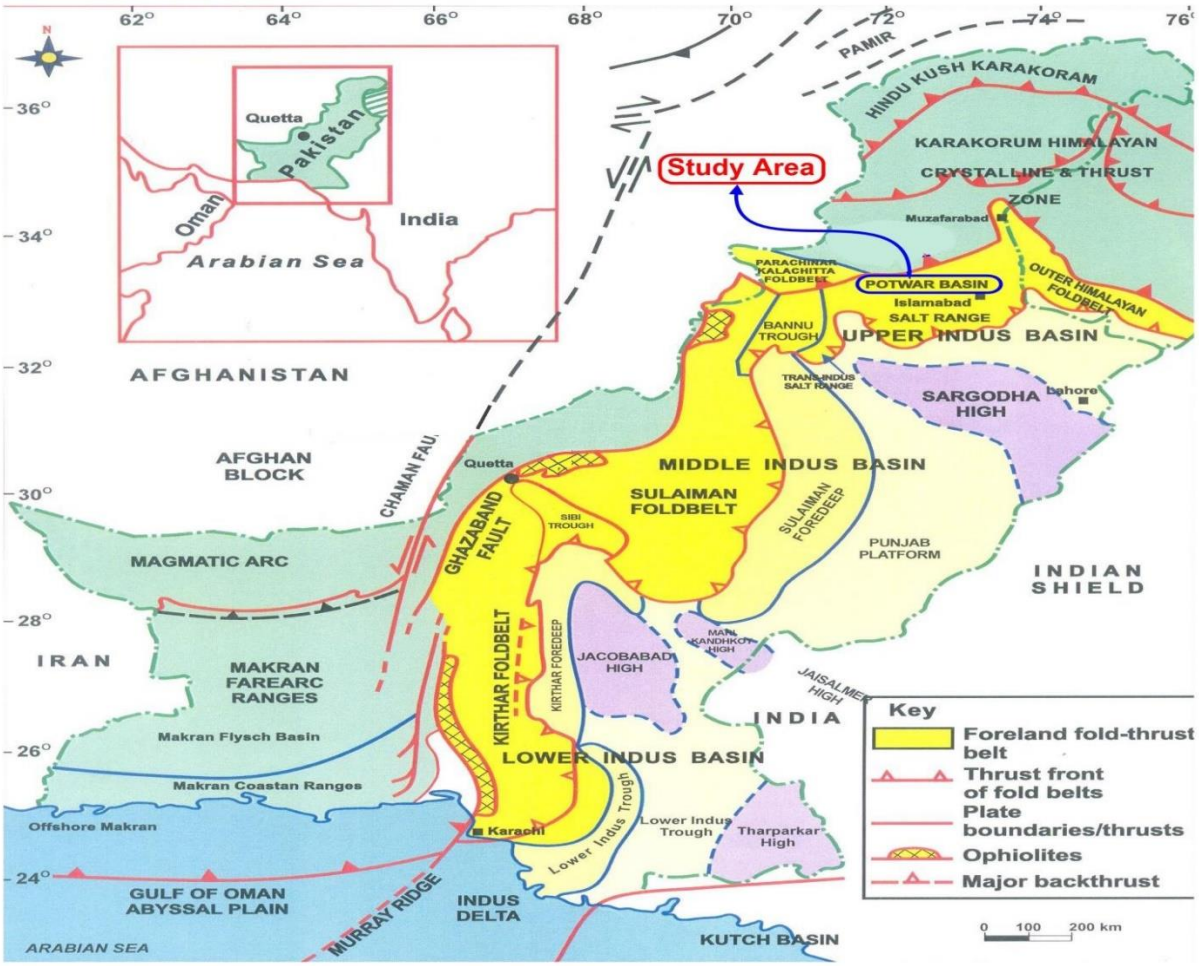

Figure 2.1: Map Showing study area and geological boundaries (Banks and Warburton, 1986).

The Potwar sub basin is bounded by the following two strike-slip and two thrust fault which are,

- Kalabagh Fault.
- Jhelum Fault.
- Salt Range Thrust.
- Main Boundary Thrust.

2.2 Tectonic of Potwar Basin:

The deformation in Potwar sub basin occurred by thrusting, with tight and occasionally overturned anticlines separated by broad synclines. The popup structures are formed mainly by thrust faults. The main faults detach on the regional plane of decollement i.e. Salt Range Formation (SRF). The eastern Potwar basin is dominated by over thrust tectonics, so mainly folds and faults are the dominated structures. The trend of most of the folds is NE-SW shown in Figure 2.2. Popup structures and snaked head structures are commonly developed in this area and these structures act as hydrocarbon traps. Domeli thrust and Salt Range thrust are the two major faults in east and south of Potwar sub basin. (Aamir and Siddiqui, 2006).

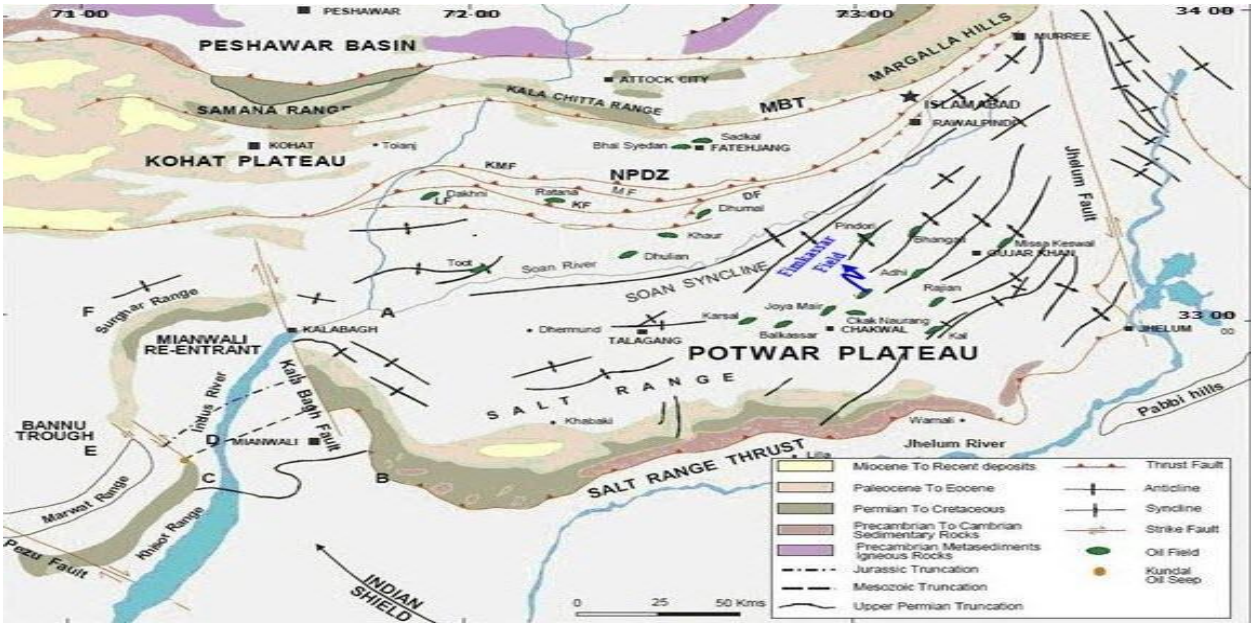

Figure 2.2: Geological and structural map of Potwar (Khan, 1986; Gee, 1989).

2.2.1 Major Faults in Potwar Basin:

Major faults of the study area are given below

- Khair-i-Murat Fault (KMF)
- Sakhwal Fault (SF)
- Kanet Fault (KF)
- Dhurnal Back Thrust (DBT)
- Mianwala Fault (MF)
- Riwat Fault (RF)

2.2.2 Major Folds in Potwar Basin:

Major folds in the study area are given below

- JoyaMair Anticline
- Mahesian Anticline
- Dhurnal Anticline

2.3 Structures in Potwar Region:

By seismic interpretation following structures are observed in a Potwar region,

- Snake head anticlines.
- Pop-up anticlines.

2.4 Stratigraphy of Eastern Potwar Basin:

Generalized stratigraphic column is shown in the Figure 2.3. Different rocks were deposited in different environments in different ages. In my study area, oldest rock penetrated is the Salt Range Formation. We have regional unconformity during Ordovician to Carboniferous in Upper Indus Basin, due to uplifting (Shami and Baig, 2002). So, Jhelum Group is dishonorably overlain by Nilawahan Group of Permian age which includes Tobra, Dnadot, Warcha and Sardahi Formations. Zaluch Group of Late Permain age was eroded or not deposited in Upper Indus Basin, late Permian to Cretaceous rocks from west to east in this basin was eroded due to significant pre-Paleocene uplift in Salt Range Potwar basin.

We have thick early Paleocene sequence due to marine transgression. In this sequence, we have Sakessar, Chorgali and Nammal Formations. Carbonates of this sequence provide oil reservoirs in this area

In Salt Range Potwar Foreland Basin (SRPFB) the Himalayan orogeny started the Eocene to Oligocene uplift and erosion (Shami and Baig, 2002). So, on the upper part of stratigraphic section we have Miocene to Pleistocene non-marine molasses deposits. It includes Rawalpindi Group (Murree and Kamlial). Molasses lay on the Lower Eocene carbonates and the southern SRPFB. These over pressured molasses act as cap rock in the southern SRPFB (Shami and Baig, 2002).

2.5 Petroleum Play:

The petroleum play of the area is very important it tell us about the Source rock, Reservoir rock and Seal/Cap rock of the area. The Stratigraphic column of the area showing these rocks is given in the Figure 2.3. The general description is given below

2.5.1 Source Rock:

Source rock is the productive rocks for hydrocarbons. The Formations which act as source rocks in the study area is Patala formation. The Patala Formation overlies the Lockhart formation conformably and its type section is in the Patala Nala in the Western Salt Range (Davies and Pinfold, 1937). It consists largely of shale with sub-ordinate marl, lime stone and sandstone. Marcasite nodules are found in the shale. The age of the Patala Formation is Late Paleocene, shown in Figure 2.3.

2.5.2 Reservoir Rock:

Reservoir rock is one of the important rock in petroleum play system that hold the hydrocarbon. The formations which act as reservoir rocks are Sakesar and lower Chorgali formation. Sakesar formation is major formation, acting as reservoir producing both Oil and Gas in Fimkassar area. It is a fractured reservoir, having negligible porosity (Bender and Raza, 1995). The formation consists of limestones of grey color and show stylolites. The age of Sakesar formation is early Eocene.

Another formation which act as a reservoir rock is Chorgali formation. The formation consists of massive dolostones, marls, nodular, extremely fissile varicolored shales, and evaporate collapse breccia. It is 80 to 90 m thick and is early middle Eocene in age Reservoir rocks are shown in Figure 2.3.

2.5.3 Seal/Cap/Trap Rock:

Hydrocarbon present in the subsurface are trap by the seal rock. In study area associated structures are pop up anticlines and snaked head structures. The formation which act as a reservoir rock in the study area is Murree formation. The clays and shales of the Murree formation provide efficient seal to Eocene reservoirs wherever it is in contact. Figure 2.3 showing the seal rock of the area.

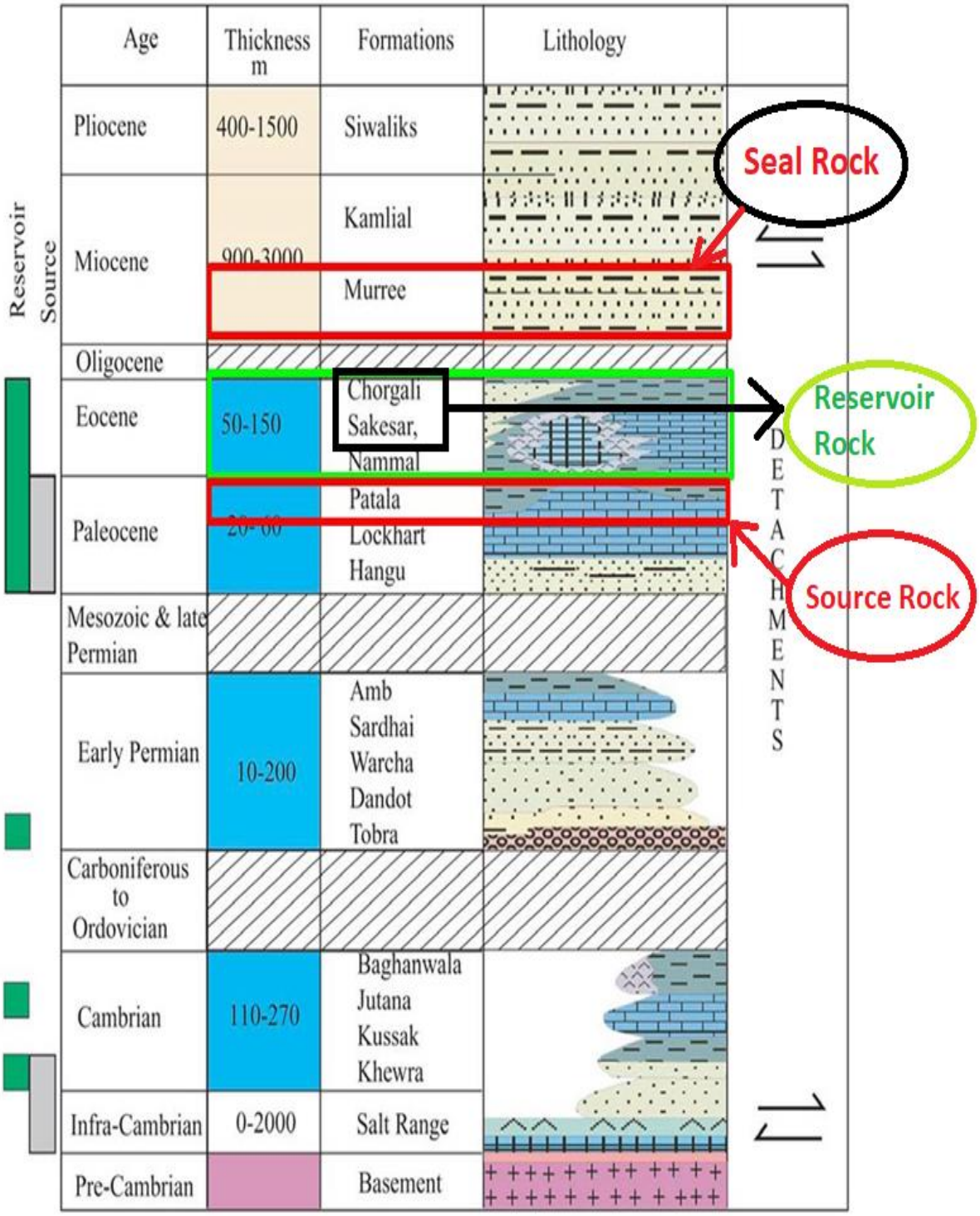

Figure (2.3): Schematic stratigraphic column of eastern Potwar (Aamir and Siddiqui, 2006).

CHAPTER # 03

SEISMIC DATA INTERPRETATION

3.1 Introduction:

Seismic interpretation models the earth structurally and stratigraphically by transforming the seismic data. Seismic interpretation determines the area of interest in perspective of hydrocarbon (Coffeen, 1986). Seismic reflectors and discontinuities are marked on the seismic section to depict the area of interest that are favorable for hydrocarbon accumulation. Some of the reflectors are not prominent and sometimes it's difficult to trace them so we must pick additional reflectors above and below the target to understand the trend of the area and our zone of interest. In last we convert the seismic section into geological section so we get the realistic structurally and stratigraphically picture of the area (Badley, 1985).

Seismic interpretation is a computer based work which is more accurate, precise and provide satisfactory results.

3.2 Structural Interpretation:

Seismic data interpretation is done on basis of geology and stratigraphy of the area. With the help of synthetic seismogram, we correlate the seismic with the formation tops within the well. In the given study, seismic interpretation is done by picking horizons in Kingdom suit and reflector is continued in all other seismic lines. Major faults are picked on the dip lines and their parts are correlated across the strike lines to map the structures throughout the area. Mistie is a major concern during interpretation, which is resolved by using of bulk shift of different time. Fault polygon is generated and by the help of this fault polygon we generate the two-way time(TWT) and depth contour maps this will show the structural inclination. The study area is in compressional regime so mainly popup and snaked head structures are present. The interpretation is performed by Kingdom Suit (8.8) and the work flow adopted in the interpretation is given below in the Figure 3.1.

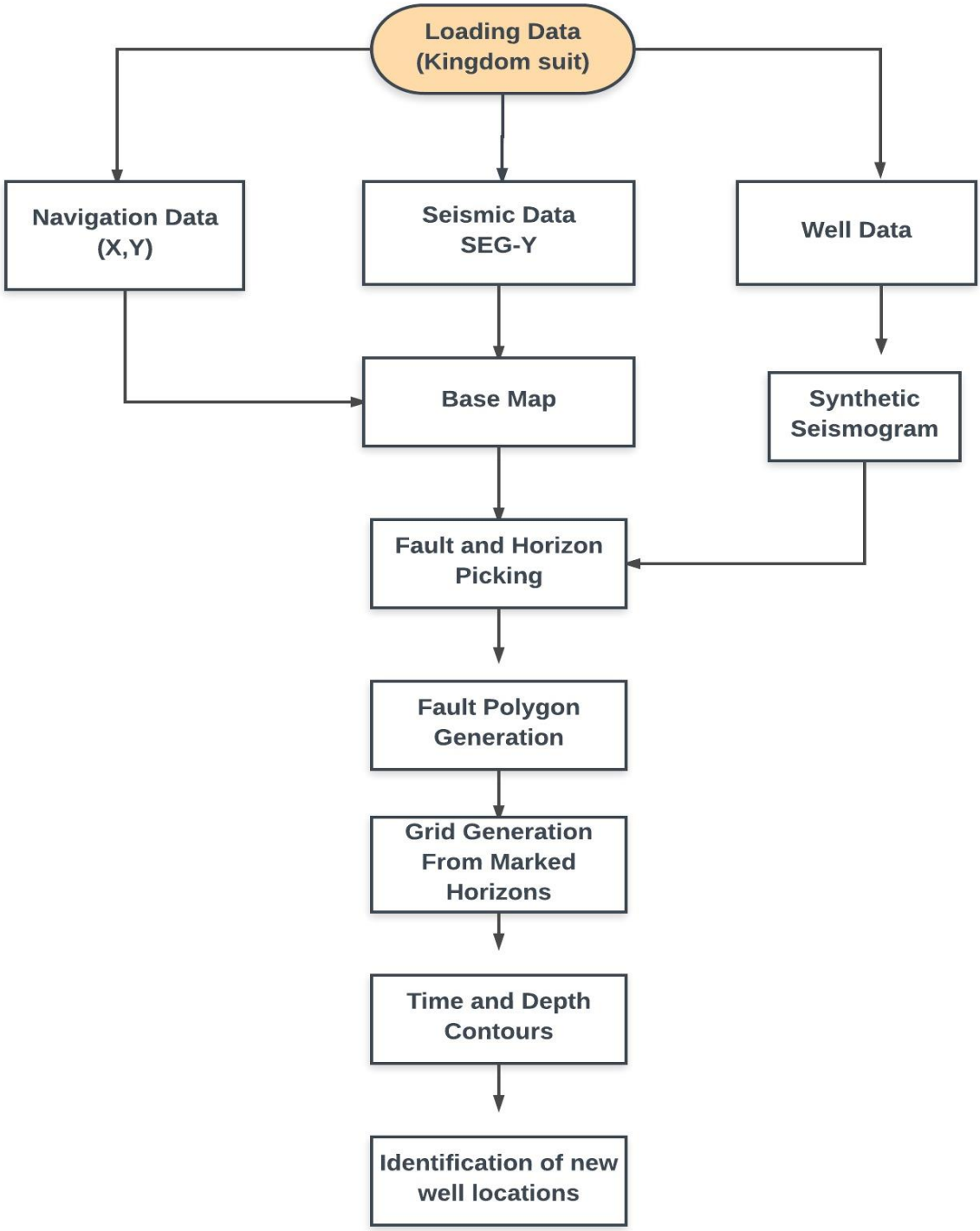

Figure 3.1: Interpretation Work Flow

3.3 Synthetic Seismogram:

Synthetic seismograms provide a crucial link between lithological variations within a drill hole and reflectors on seismic profiles. With the help of "Turkwal-01" well data, I construct the synthetic seismogram shown in Figure 3.2 to mark the horizons crossing the site. Synthetic seismograms link the drill hole geology to seismic sections (Handwerger et al., 2004). With the help of sonic and density log we get velocity and density, by multiplying velocity and density we get acoustic impedance which then converted to reflectivity series (R.C). RC then convolved with the source wavelet to get synthetic seismogram. By generating the synthetic seismogram, we identify the origin of seismic reflectors (Handwerger et al., 2004)

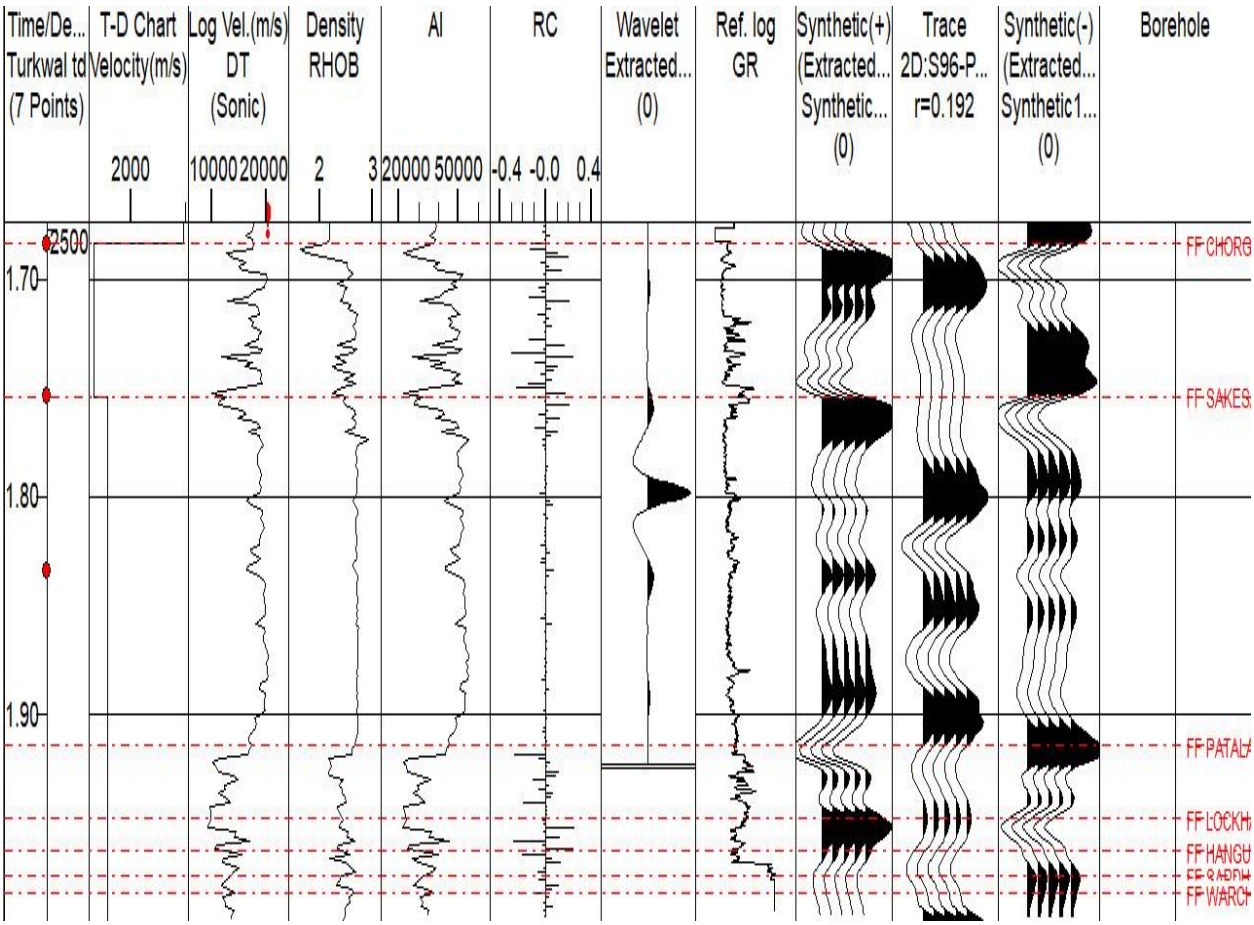

Figure 3.2: Synthtic siesmogram developed at Turkwal-01 well

3.4 Interpretation of Seismic Lines:

It includes various steps which are listed below one by one

3.4.1 Identification of Faults:

On basis of the Geology of the study area I came to know that the study area lies in compressional regime and reverse and thrust faults should be marked so different faults are marked which are shown in the Figure 3.3 and Figure 3.4 respectively.

3.4.2 Marking of Seismic Horizon:

Primary task of the interpretation is the identification of various horizons. For this purpose, good structural and stratigraphic knowledge of the area is required (McQuillin et al, 1984). Thus, during interpretation, I marked three horizons on basis of the well tops obtained from synthetic seismogram at the well Turkwal-01. These horizons are named (Chorgali, Sakesar and Patala) and they show high reflection on the seismic section and easy to be picked. The horizons marked on the seismic lines are shown in the Figure 3.3 and Figure 3.4 respectively.

3.5 Interpreted Seismic Sections:

The two dip lines are interpreted i.e. S96-PW-04, G884-FMK-106, S96-PW-02 which are shown in the Figure3.3, Figure3.4 and Figure3.5 respectively. Three seismic horizons named (Chorgali, Sakesar of Eocene age and Patala of Paleocene age) are marked on basis of the well tops and furthermore confirmed by synthetic seismogram.

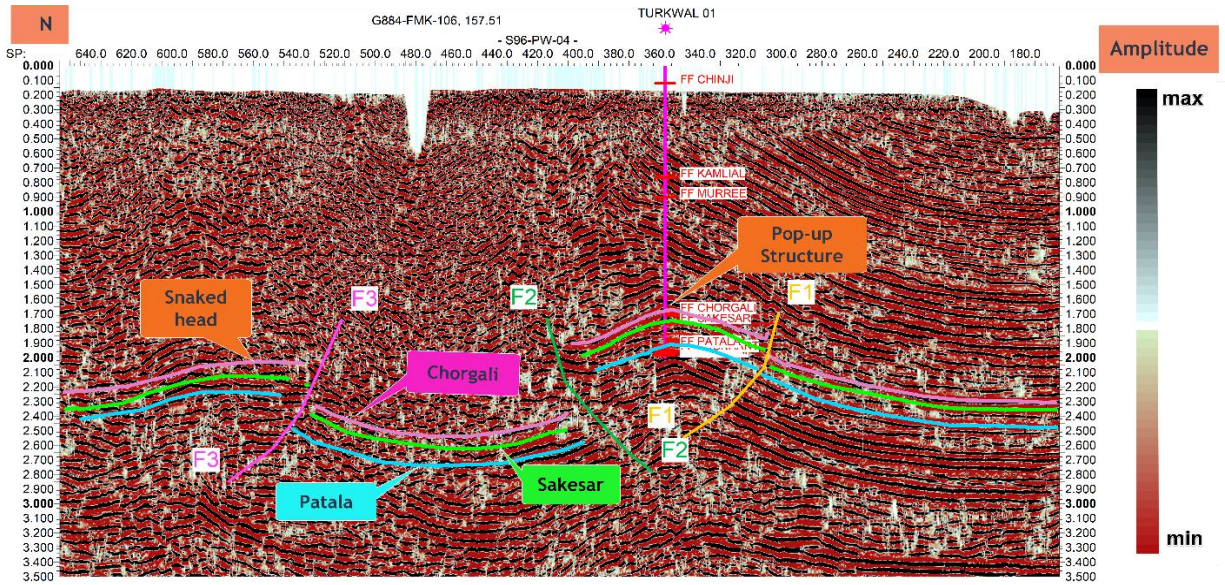

Figure 3.3: Interpreted seismic line S96-PW-04.

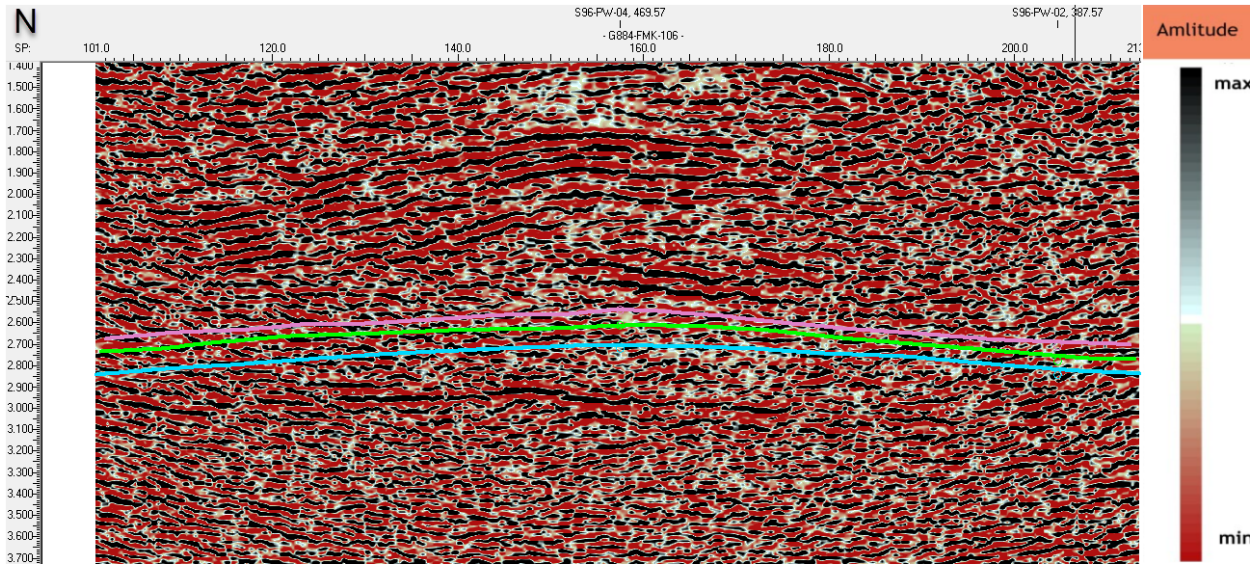

Figure 3.4: Interpreted seismic line G884-FMK-106.

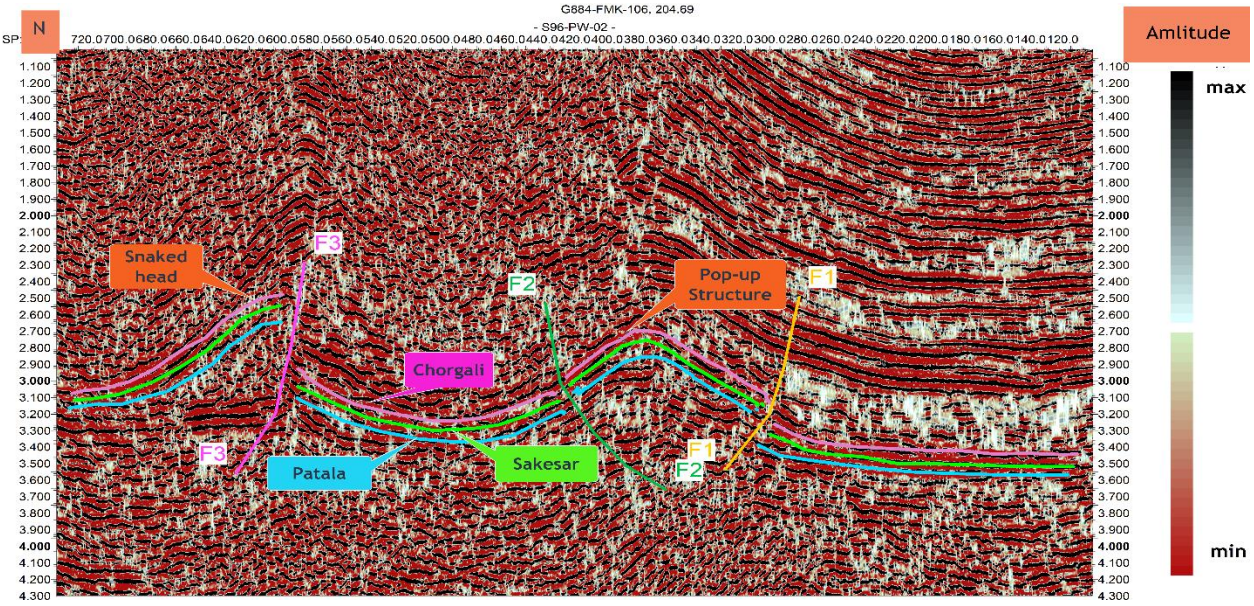

Figure 3.5: Interpreted seismic line S96-PW-02.

Seismic interpretation of lines i.e. S96-PW-04, G884-FMK-106, S96-PW-02 which are shown in the Figure3.3, Figure3.4 and Figure3.5 respectively shows that mainly popup anticline and snaked head structures are present in the study area.

3.6 Fault Polygon Generation:

A fault polygon represents the lateral extent of dip faults having same trend. Fault polygon show the sub-surface discontinuities. To generate fault polygon, it is necessary to identify the faults and their lateral extent if one finds that the same fault is present on all the dip lines, then all points (represented by a "x" sign by Kingdom software) can be manually joined to make a polygon. For time and depth contouring fault polygon generation is very important. The reason that if fault is not converted into polygon the software doesn't recognize it as a barrier or discontinuities, thus represent a false picture of the subsurface. After construction of fault polygons, the high and low areas on a horizon become obvious. Fault polygons are constructed for all formations i.e. Chorgali, Sakesar and Patala formation and these are oriented in NE-SW direction. The fault polygon of Chorgali formation is shown in Figure 3.6.

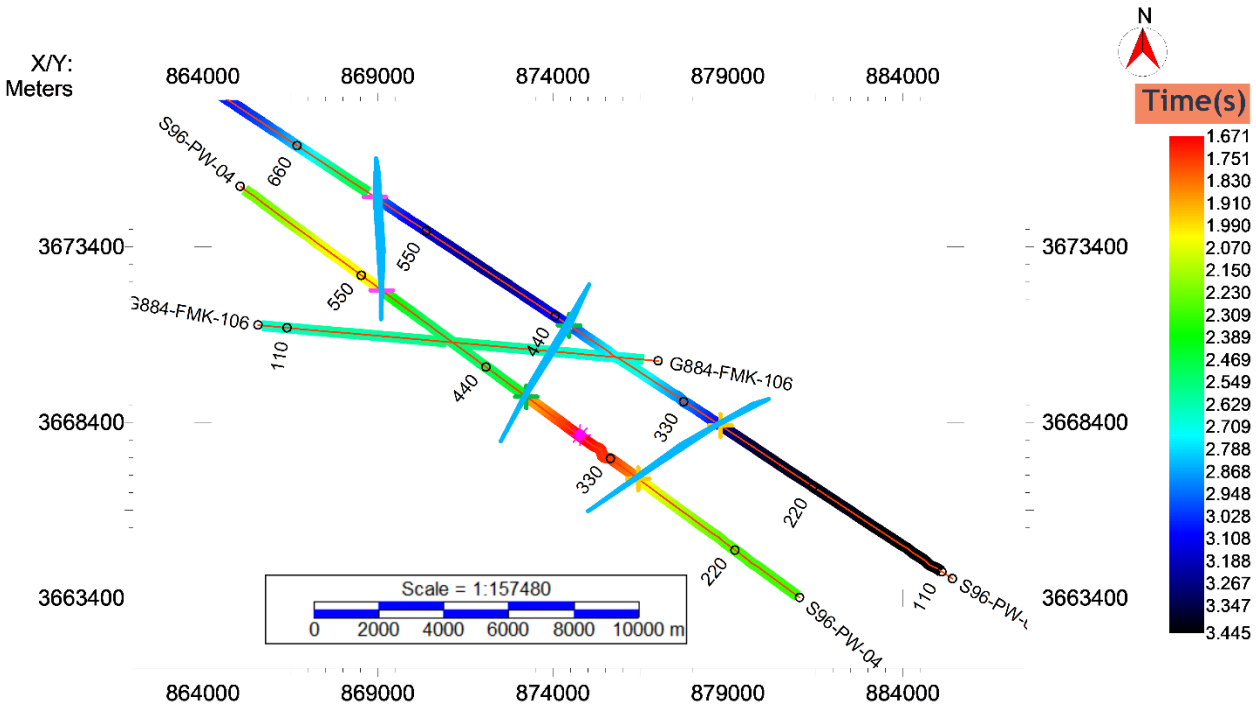

Figure 3.6: Polygon's orientation on base map.

3.7 Contour Maps:

Mapping is part of the interpretation of the data. Contour maps are constructed on basis of seismic interpretation. The contours are the lines of equal time or depth wandering around the map as dictated by the data (Coffeen, 1986). Contouring represents the 3D earth on a 2D surface. The

spacing of the contour lines is a measure of the steepness of the slope i.e. closer the spacing, steeper the slope.

3.8 Time and Depth Contour Maps of Chorgali Formation:

The time and depth map of Chorgali Formation are generated on the base map along with wells shown in Figure 3.7 and 3.8. The polygon F1, F2, F3 shows dipping in NE-SW direction. The TWT contour map of Chorgali Formation is shown in figure. The contour interval for time contours is set as 50msec and that of depth contour is 80m. The structural variation in these contours is can be interpreted by using color bar and legends. The light blue color ranges from (1.67s-1.882s) shows the shallowest part and light orange color approaches from (2.881s-3.038s) shows the deepest part. The time and depth contour map are shown in Figure 3.7 and 3.8.

For depth contouring I used software built-in function, I gave time from the seismic data and by using average velocity depth was automatically calculated. The negative value in the depth contour map are due to the selection of subsea as a reference point.

The depth variation in contour map is interpreted by using color bar shown in figure. The light blue color from (2821m-3034m) shows the shallowest part while orange color from (4730m-5154m) shows the deepest part.

The following interpretations are made from these time and depth contours shown in the figures given below

- The interpreted structure for Chorgali Formation is a pop-up anticline and snaked head structure.
- The pop up anticline is bounded by thrust faults F1 and F2 and snaked head structure is formed due thrust fault F3. The time and depth contour map are shown in Figure 3.7 and Figure 3.8 respectively.

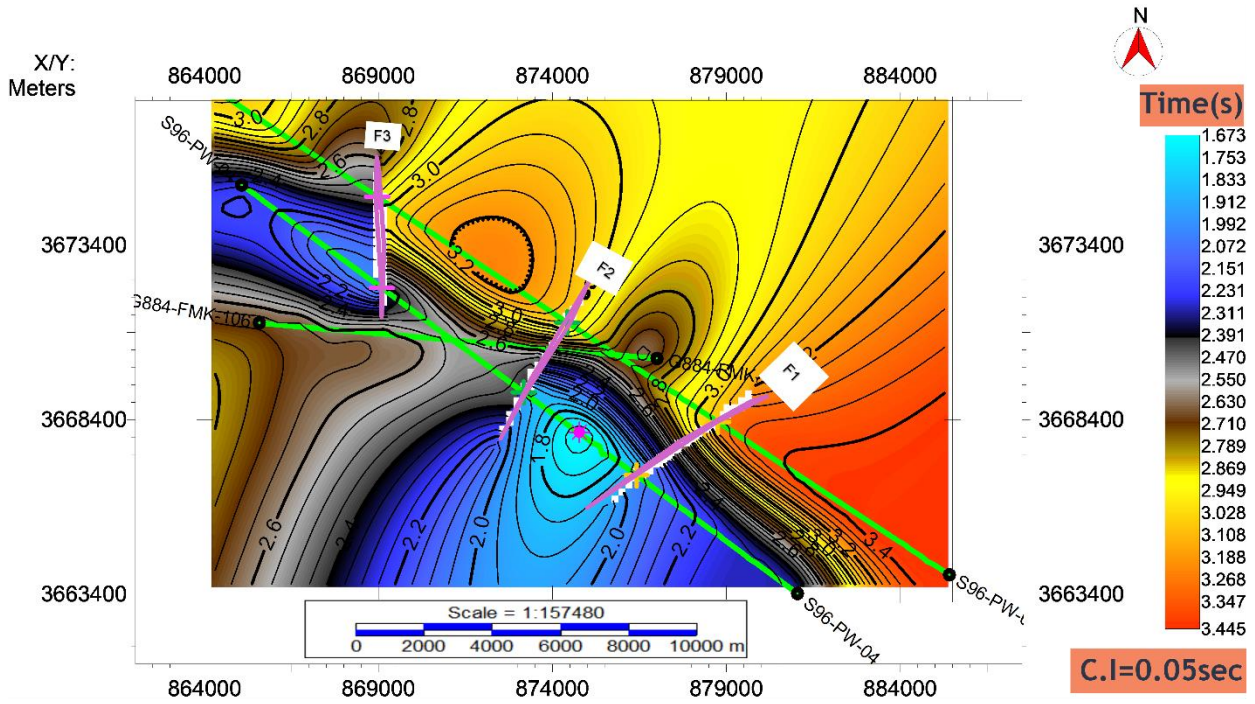

Figure 3.7: TWT contour map of Chorgali Formation.

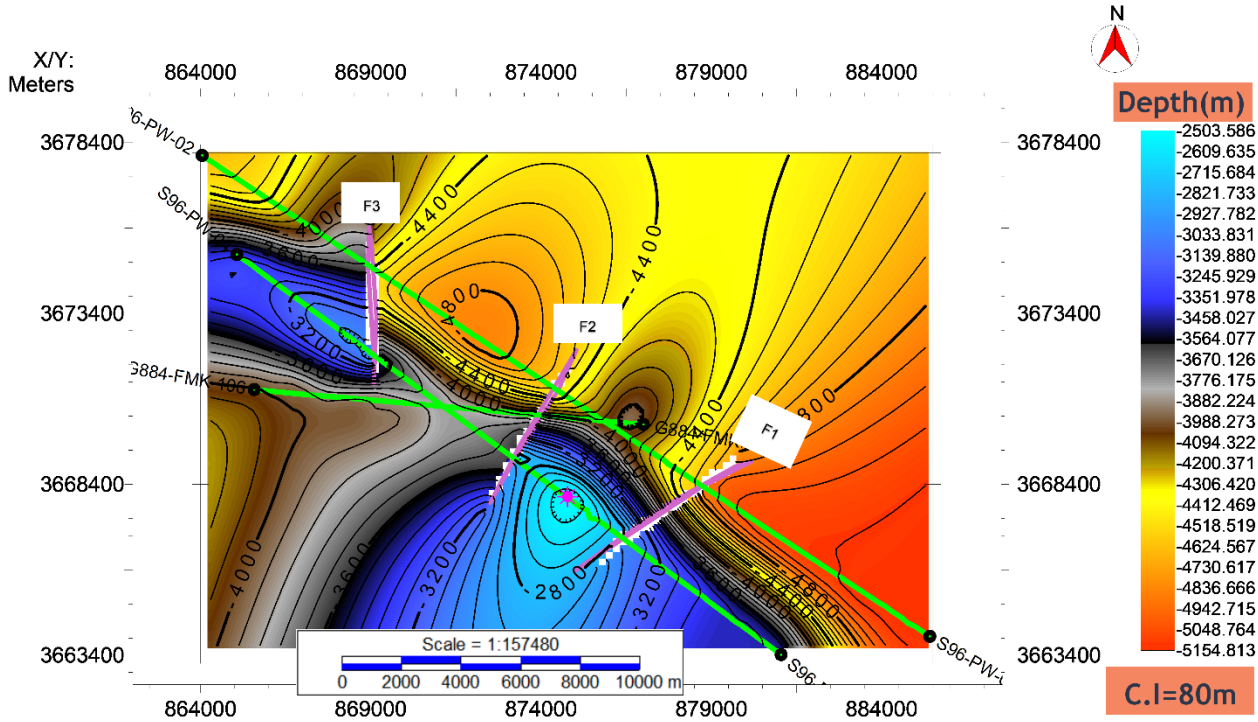

Figure 3.8: Depth contour map of Chorgali Formation.

3.9 Time and Depth Contour Map of Sakeser Formation:

The time and depth map of Sakeser Formation are generated on the base map along with wells and their corresponding fault polygons shown in figure. The polygons F1, F2 and F3 are dipping in NE-SW direction. The TWT contour map of Sakesar Formation is shown in Figure 3.9. The contour interval for time contours is set as 50ms and that of depth contour is 80m. The structural variation in these contours can be interpreted by using color bar and legends. The light blue color ranges from (1.741s-1.954s) shows the shallowest part and yellow to orange color ranges from (2.950s-3.306s) shows the deepest part. The contour map helps us to mark the zone of interest. Sakesar Formation is the second zone of interest and one of the major potential reservoirs after Chorgali. Here at this level similar fault polygon are observed which indicates a presence of same faults on both Formations. Hence blue color ranges from (1.741s-1.954s) shows the highest peak or elevated part i.e. most favorable area for hydrocarbon extraction. The depth variation in contour map is interpreted by using color bar shown in Figure 3.10. The light blue color from (2542m-2750m) shows the shallowest part while orange color from (4724m- 5140m) shows the deepest part.

Time and depth contour map of Sakesar Formation are given below in Figure 3.9 and Figure 3.10 respectively.

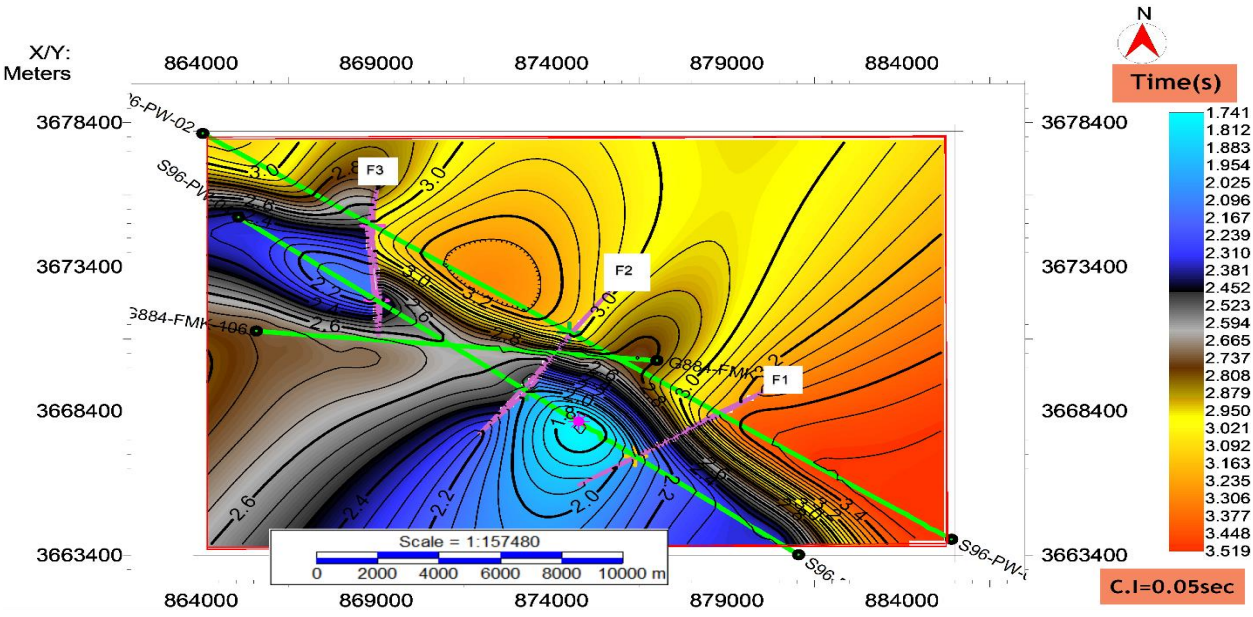

Figure 3.9: TWT contour map of Sakesar Formation.

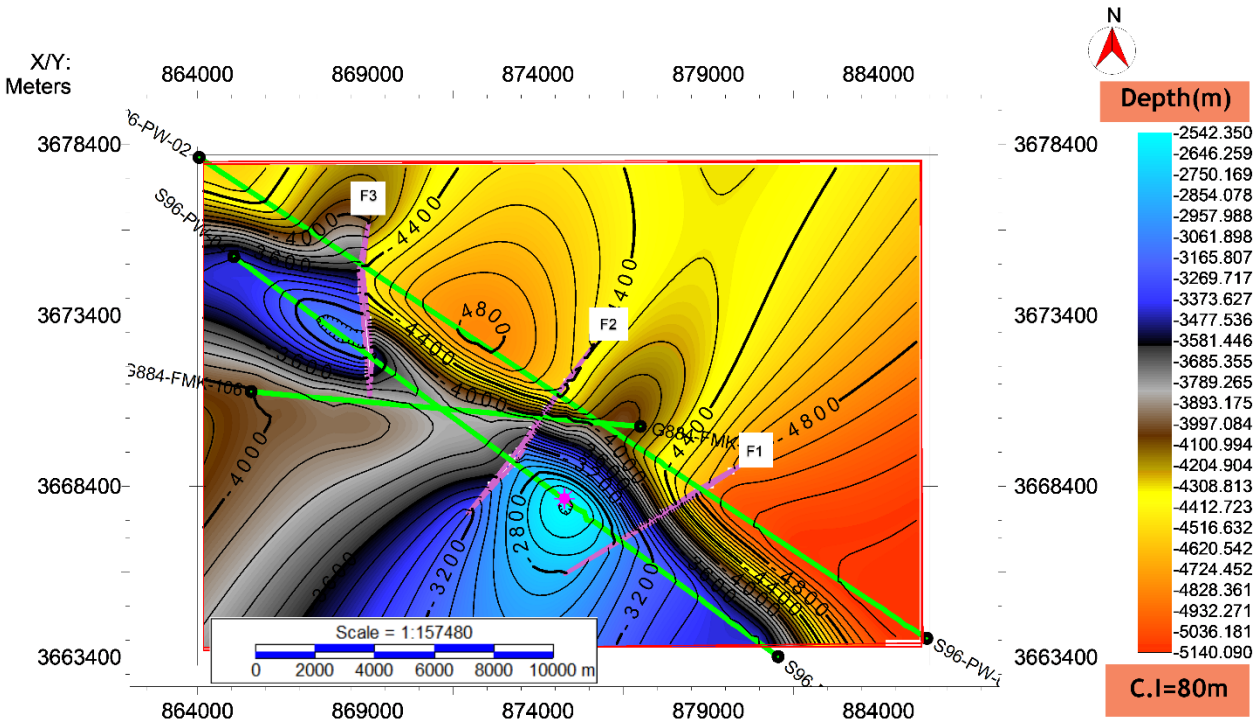

Figure 3.10: Depth contour map of Sakesar Formation.

3.10 Time and Depth Contour of Patala Formation:

Patala Formation can act as both reservoir as well as source rock. The time and depth contour map is generated can be interpreted as by two other Formations using color bar. The time and depth maps can be interpreted by using same techniques as we have done in previous Formations. The contour map shown in figure almost gives same structure interpretation as of previous two Formations discussed above. The TWT contour map can be interpreted from the color bar. The light blue color ranges from (1.906s-2.039s) shows the shallowest part or elevated part is our zone of interest. It is interpreted as pop-up structure because value of time is decreasing as we move outward. The depth map of Patala Formation is also constructed by same procedure that we have discussed above. The depth map of Patala Formation can also have interpreted by using color bar. The depth value ranges from (2665.281m-2852.126m) shown by light blue color and depth values ranges from (4720m-5000.845m) represents the deeper part which are shown by orange color.

Time and depth contour map of Patala Formation are given below in Figure 3.11 and Figure 3.12 respectively.

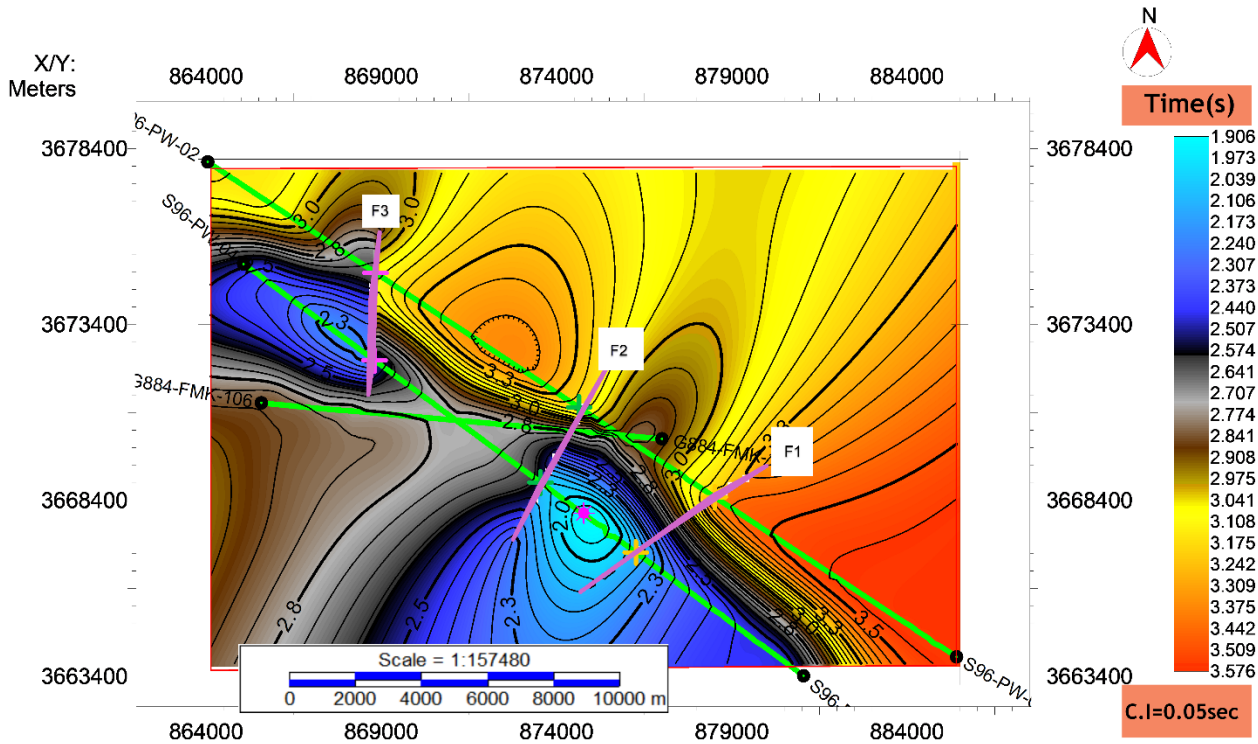

Figure 3.11: TWT contour map of Patala Formation.

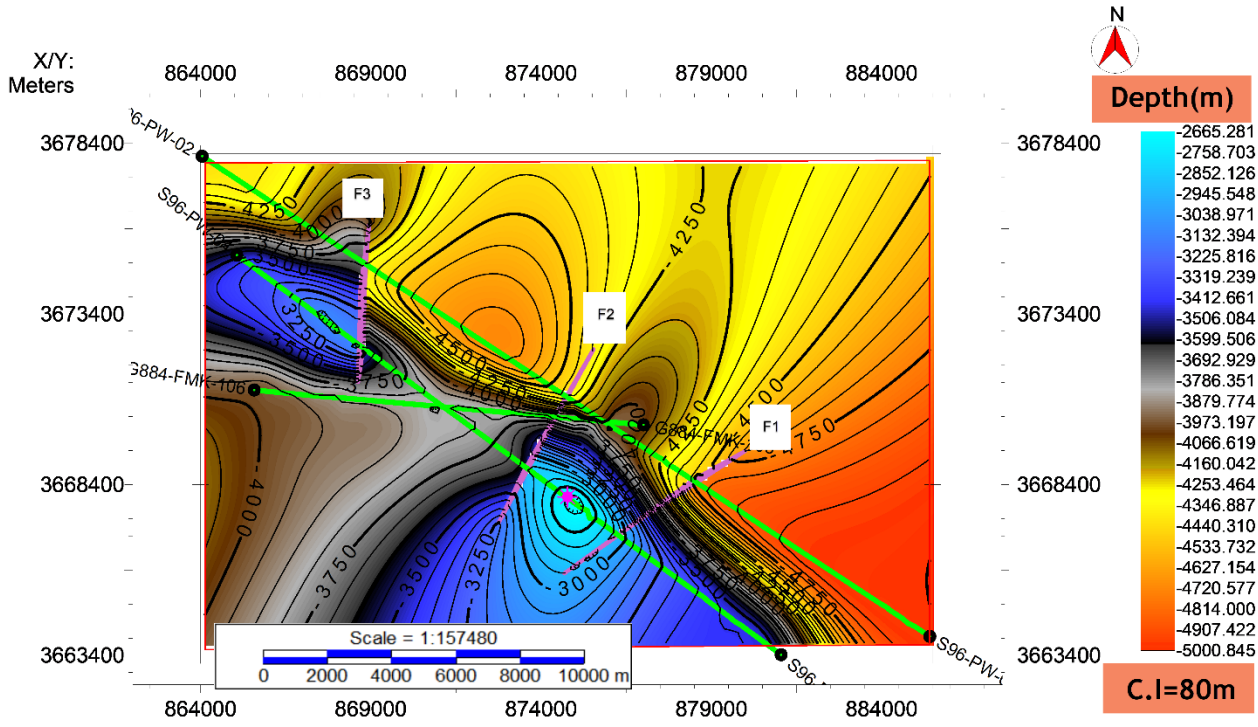

Figure 3.12: Depth contour map of Patala Formation.

3.11 Identification of Well Location:

The purpose of generating contour map is to find to determine the area where hydrocarbons accumulate. The hydrocarbon mostly accumulates in the regions of low pressure and permeability. Ideally these regions are hinge of the anticlines. In real case, the hinge of anticline is also structurally disturbed and there is a risk of drilling in that location (Coffeen, J.A., 1986). In our study area, the pop-up anticline structure is associated with thrust faults and other faults in adjacent area provide low pressure areas, so may be marked as proposed possible Well locations. The locations are identified over depth contour maps illustrated below in Figure 3.13, 3.14and 3.15 respectively.

3.11.1 Lead-01:

The lead is a three-way dip structure comprised of snaked head structure. Lead-01 is marked based on contour closure, shallow time and shallow depth. Two side of closure is controlled by thrust fault and third side is controlled by dip of the structure. Lead-01 at Chorgali, Sakesar and Patala formation is shown in Figure 3.13, 3.14 and 3.15 respectively.

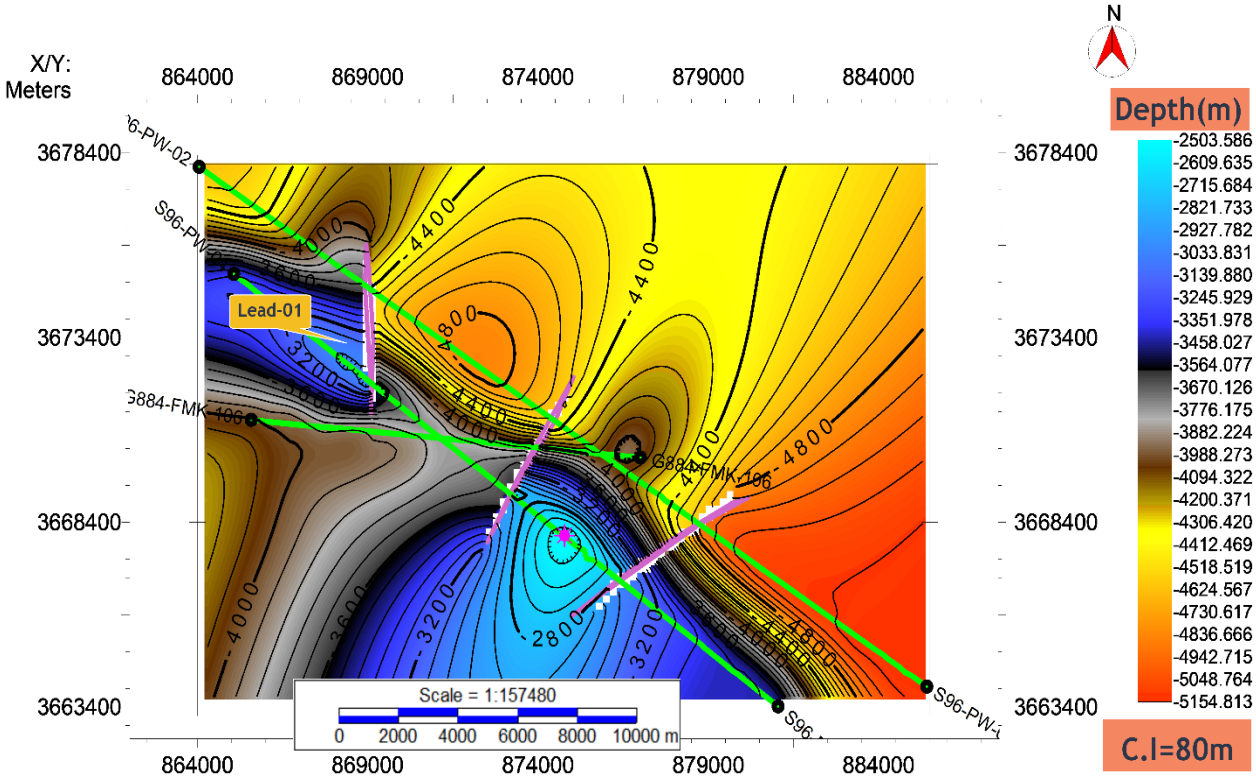

Figure 3.13: Identification of leads of Chorgali Formation.

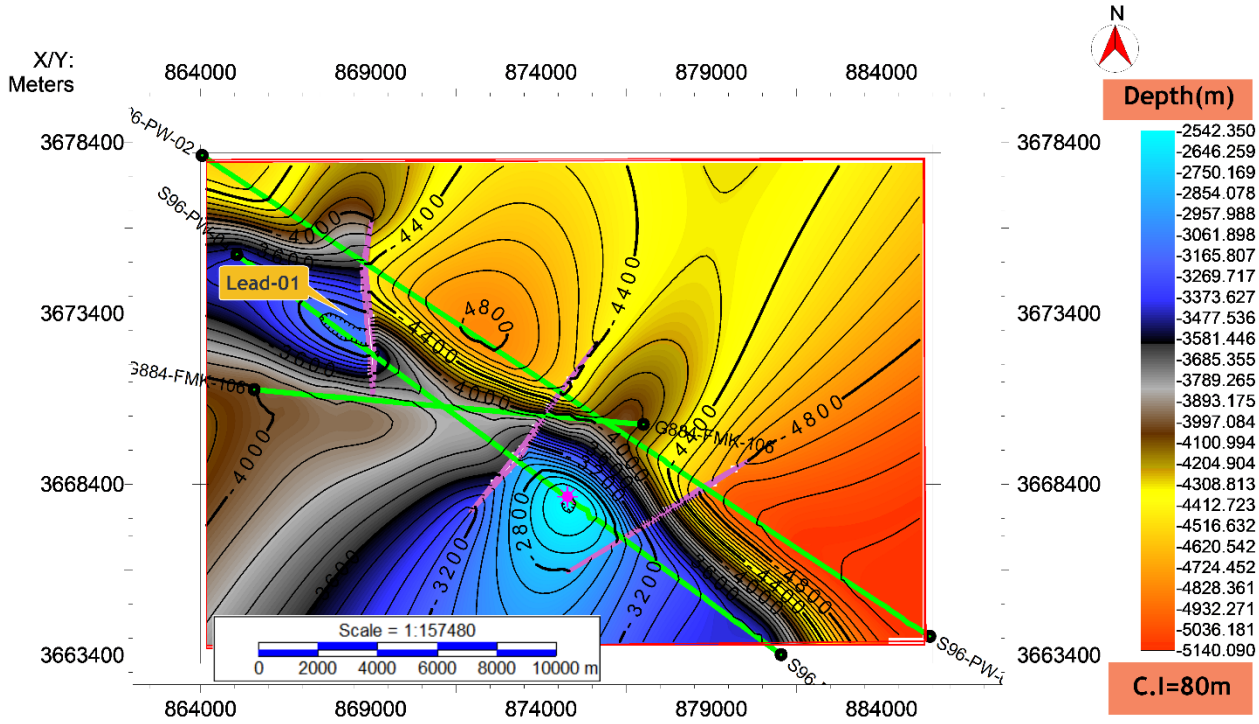

Figure 3.14: Identification of leads of Sakesar Formation.

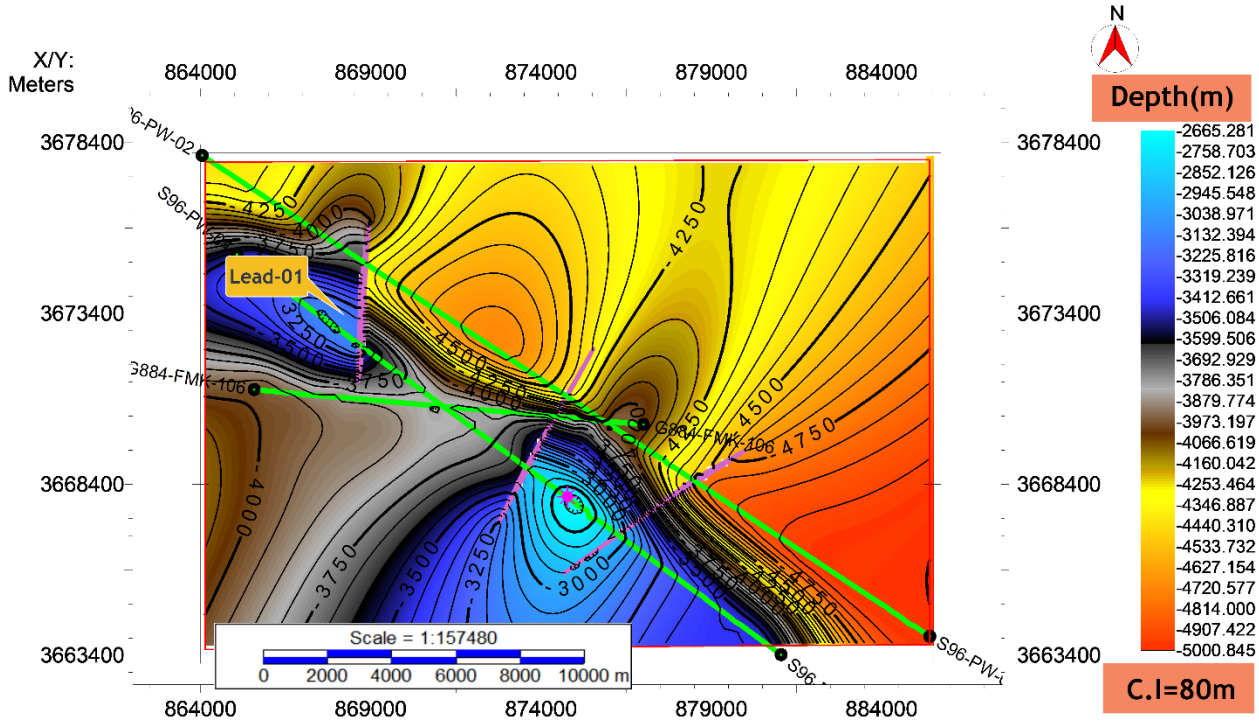

Figure 3.15: Identification of leads of Patala Formation.

3.12 Seismic Attributes:

For the better visualization and accuracy of the seismic interpretation seismic attributes are applied on the seismic data. Seismic attribute help in the prediction of prospect zones for hydrocarbon accumulation. The principal objectives of the Seismic attributes are to interpret faults, channels, recognize depositional environments, and unravel structural deformation history more rapidly and efficiently (David Oyeyemi and Phillips Aizebeokhai,2015).

3.12.1 The Classification of Attributes:

Attributes can be computed from pre-stack or from post-stack data, before or after time migration. Here we give a classification of the attributes

- **Pre-Stack Attributes:**

Input data are CDP or image gather traces. They will have directional (azimuth) and offset related information. These computations generate huge amounts of data; hence they are not practical for initial studies. However, they contain considerable amounts of information that can be directly related to fluid content and fracture orientation. AVO, velocities and azimuthal variation of all attributes are included in this class (Taner,2001).

- **Post-Stacking Attributes:**

Stacking is an averaging process that eliminates information about offset and azimuth. The input data can be either stacked CDP or migrated. It should be noted that data migrated over time will maintain their temporal relationships, so time variables, such as frequency, will also retain their physical dimensions. For the sections transmitted at depth, the frequency is replaced by the wave number, which is a function of the propagation velocity and the frequency. Post-stack attributes are an easier-to-manage approach for observing large amounts of data in initial reconnaissance surveys (Taner,2001).

  - **Instantaneous Attributes:**

    Instantaneous attributes are computed sample by sample, and represent instantaneous variations of various parameters. Instantaneous values of attributes such as trace envelope, its derivatives, frequency and phase may be determined from complex traces (Taner,2001).

- **Wavelet Attributes:**

This class comprises those instantaneous attributes that are computed at the peak of the trace envelope and have a direct relationship to the Fourier transform of the wavelet near the envelope peak. For example, instantaneous frequency at the peak of the envelope is equal to the mean frequency of the wavelet amplitude spectrum. Instantaneous phase corresponds to the intercept phase of the wavelet. This attribute is also called the "response attribute". (Bodine, 1984).

- **Physical Attributes:**

Physical attributes refer to physical qualities and quantities. The magnitude of the trace envelope is proportional to the acoustic impedance contrast; Frequencies refer to bed thickness, wave diffusion, and absorption. The instantaneous and average velocities are directly related to the properties of the rocks. Therefore, these attributes are mainly used for lithological classification and reservoir characterization (Taner,2001).

- **Geometric Attributes:**

The geometric attributes describe the spatial and temporal relationship of all other attributes. The lateral continuity measured by semblance is a good indicator of bedding similarity as well as discontinuity. Bedding dips and curvatures give depositional information. Geometrical attributes are also of use for stratigraphic interpretation since they define event characteristics and their spatial relationships, and may be used to quantify features that directly assist in the recognition of depositional patterns, and related lithology.

3.12.2 Application of Seismic attributes on the seismic line:

- **Trace Envelope (Reflection Strength):**

Trace envelope, also called as reflection strength, represents the total instantaneous energy of the complex trace which is independent of the phase and is computed as the modulus of the complex trace (Taner, 2001).

This attribute is mainly useful in identifying:

- Bright spots, possible gas accumulation.
- Sequence boundaries.
- Thin-bed tuning effects

- Major changes in depositional environment
- Spatial correlation to porosity and other lithologic variations

This attribute is extracted for seismic line S96-PW-04 shown in Figure 3.16, to see the major changes in lithologies. Even negative reflection coefficients such as limestone formation overlaid on clayey formation would generate a positive response in this attribute.

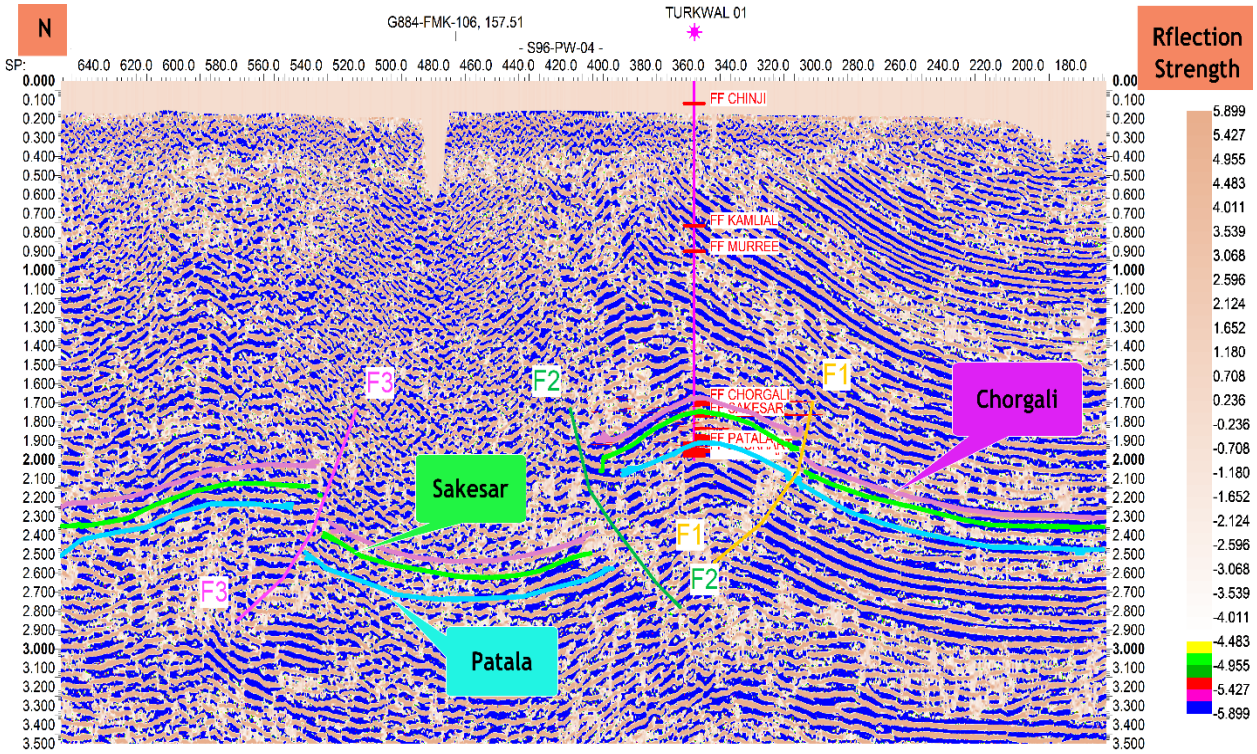

Figure 3.16: Trace envelop attribute extracted on line S96-PW-04.

The extracted Trace envelop attribute on line that is shown in the Figure 3.16 from NW to SE thickness of reservoir consisting of the limestone decreases show the less rate of sedimentation and this attribute indicates the vertical discontinuity and the lateral continuity, it is visible from the figure towards NW it shows the high hydrocarbon potential as compared to the SE which is the shale out portion.

➢ **Average Energy:**

Average Energy attribute is the sum of the squared amplitudes divided by the number of samples within the specified window used (Taner, 2001). In this study, seismic attributes are extracted using seismic data domain based classification. This attribute is computed for

seismic line S96-PW-04 shown in Figure 3.17. The wavelet attributes are computed at the peak of the envelope, which represent the attributes of the wavelets within a zone defined by the trace envelope minima. These attributes indicate spatial variation of the wavelets and therefore relate to the response of the composite group of individual interfaces below the seismic resolution. The attribute has a blocky response and individually highlights the reservoirs Chorgali and Sakesar as shown in the Figure 3.17.

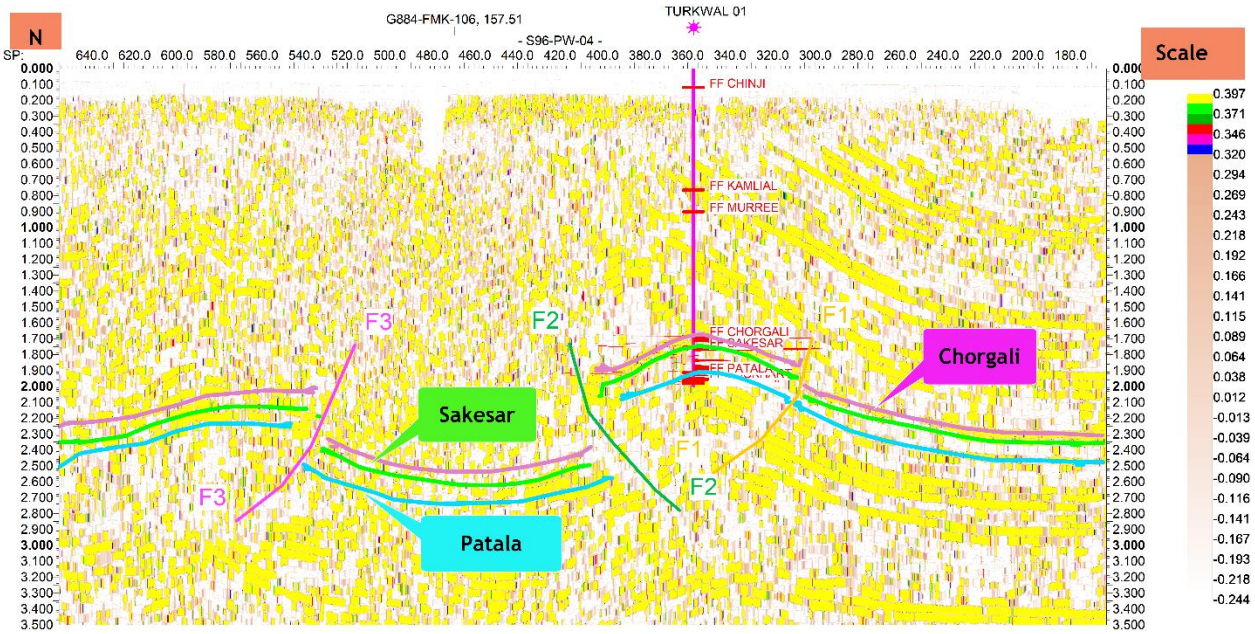

Figure 3.17: Average energy attribute extracted on line S96-PW-04.

The extracted average energy attribute on line that is shown in the Figure 3.17 toward NW sedimentation rate is higher, preservation is more, more compacted strata, high velocity, high acoustic impedance, more strong reflection and more HC effect as compared to the south-eastern side. In general, average energy give us the information about the:

- Lithology.
- Depositional environment.
- H.C effect.
- Porosity/Sedimentation rate.

CHAPTER # 04

SPECTRAL DECOMPOSITION

4.1 Introduction:

Spectral decomposition of seismic data is a mathematical tool of transforming seismic data from time domain to time vs frequency domain. It converts one dimensional seismic trace in time domain to two-dimensional time vs frequency domain representation, thus provides information on variation of frequency with time. In a similar way, it converts two-dimensional seismic section to three-dimensional representation, third axis being frequency. The frequency domain representation of seismic data illustrates many features that are not apparent in time domain representation and hence spectral decomposition serves as a useful tool for seismic interpreters (Khonde et al., 2013).

4.2 Preamble:

Early work on spectral decomposition was performed by Greg Partyka. Partyka used Short-time Fourier transform (STFT) based spectral decomposition to analyse seismic features. He used spectral decomposition for imaging and mapping temporal bed thickness and geologic discontinuities in 3D seismic data.

4.3 Methodology:

The concept behind spectral decomposition is that the seismic reflection from a thin bed has a characteristic expression in the frequency domain that is indicative of its thickness in time. A typically seismic trace contains information from multiple subsurface layers and just one single thin bed. The combined seismic response from these multiple subsurface layers usually results in a complex tuned reflection which has a unique frequency domain expression. To resolve these thin beds, spectral decomposition can be used (Partyka et al., 1999).

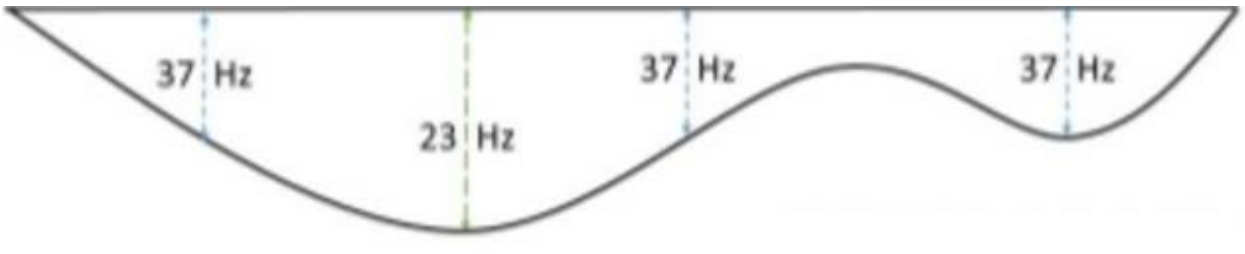

Figure 4.1: Different seismic response at different frequencies much more seismic detailed can be ascertained with the 37 Hz iso-frequency data set as compared to 23 Hz (Partyka et al., 1999).

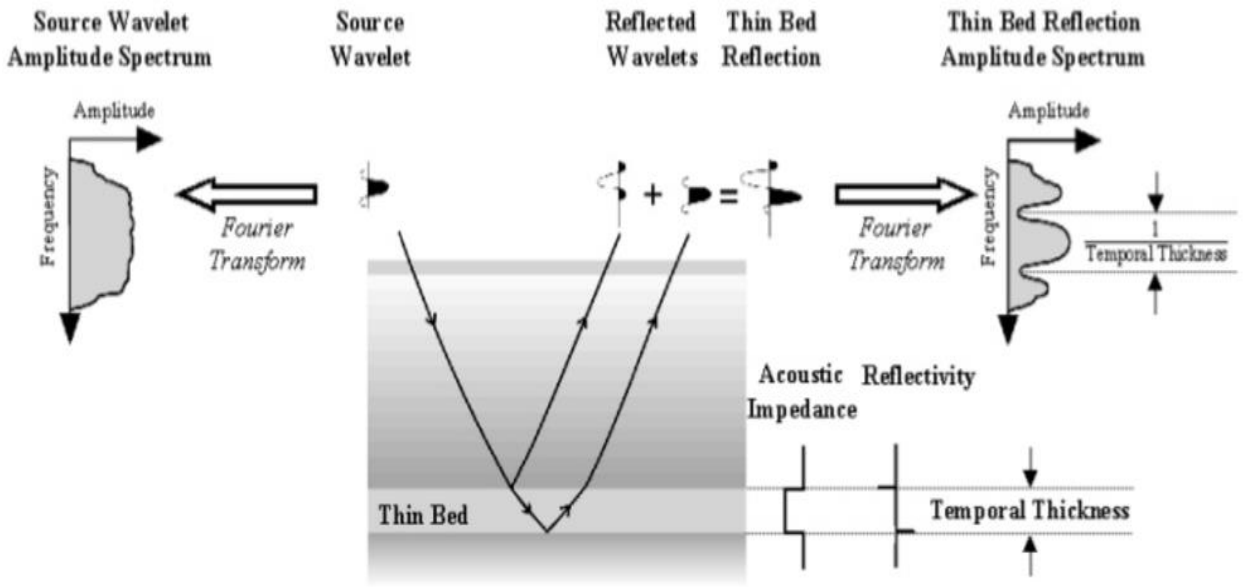

Figure 4.2: Spectral decomposition used to identify thin beds through analysis of the frequency spectrum in a short window around the time of the bed (Partyka et al., 1999).

Spectral decomposition is used to breakdown the seismic survey into its component frequencies. When determining which frequencies to extract from the dataset, it's best to use an octave scale to avoid potential harmonic (seeing the same information at multiple of its base frequency).

4.4 Application of Spectral Decomposition:

Spectral Decomposition is mainly useful in identifying

- Identifying Minor Faults.
- Identifying prospect hydrocarbon zones.

4.4.1 Identifying Minor Faults:

In this study, based on the 2D seismic data from the Fimkassar area, spectral decomposition is used for identifying minor faults. The phase tuning cube is used for interpreting fault planar variation and the common frequency cubes are used for describing the spatial features of faults. Integrating both the phase tuning cube and the common frequency improves the reliability of fault identification (Wei and X.D, 2010).

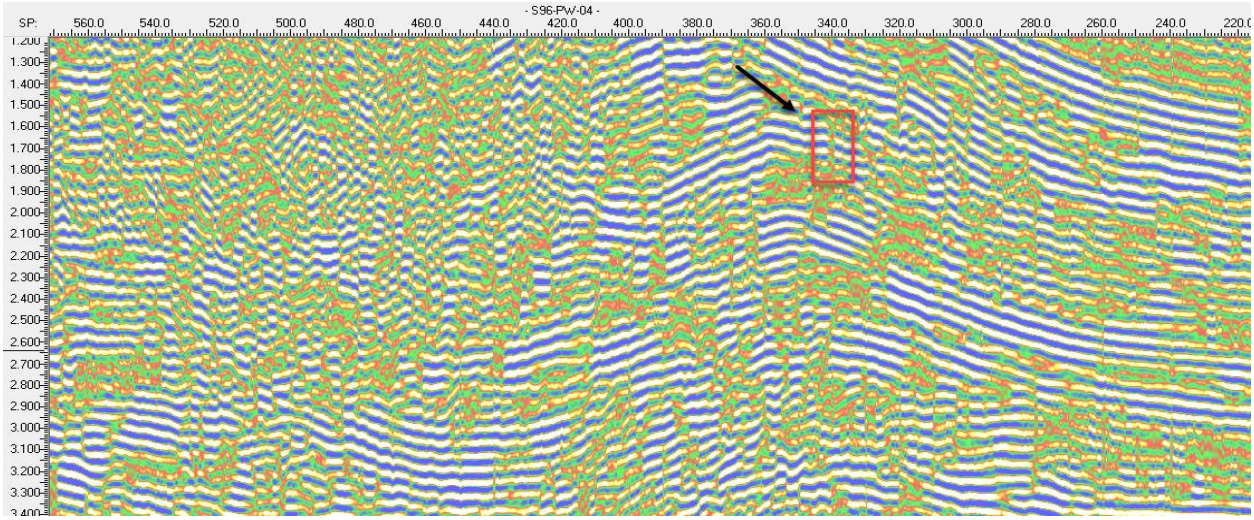

Figure 4.3: Shows minor fault at dominant frequency of 37.3 Hz.

To improve the reliability of identifying minor faults, it is necessary to evaluate seismic data quality. Figure 4.3 shows the seismic data. The frequency band of the seismic data is 10-80 Hz and the dominant frequency is 37.3 Hz, which is beneficial for using spectral decomposition to identify minor faults.

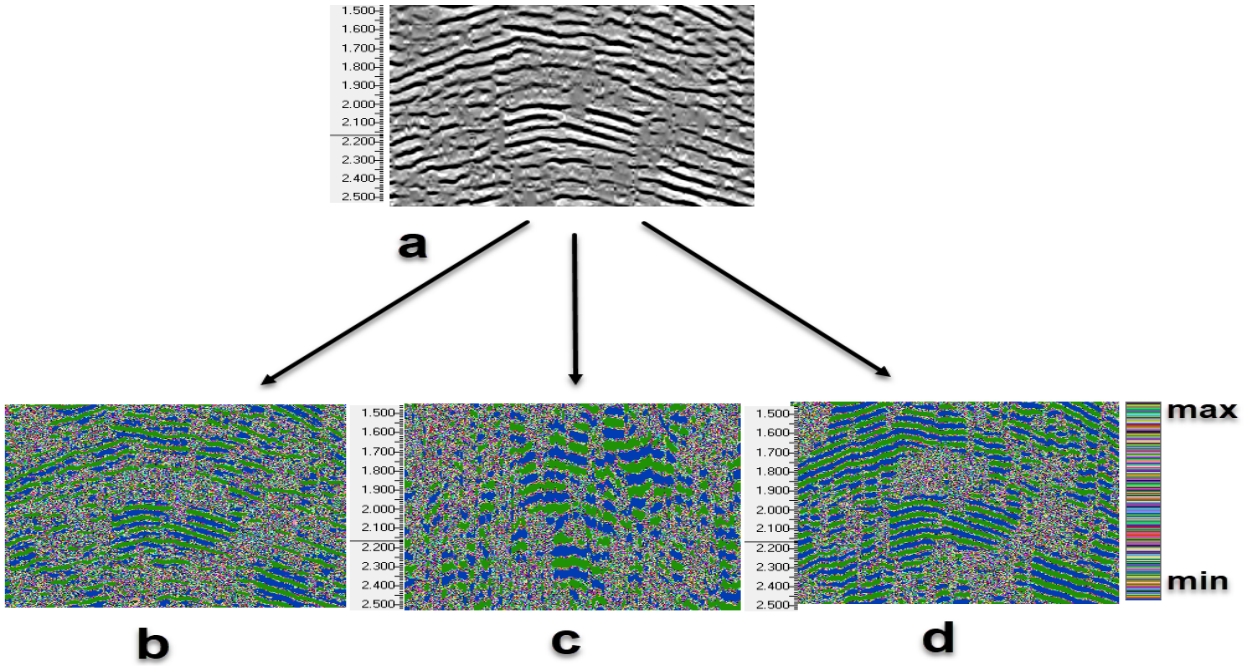

Figure 4.4: Comparison with seismic sections transformed by different spectral decomposition method. (a: original seismic trace, b: seismic section at 10 Hz, c: seismic trace at 19.3 Hz, d: seismic trace at 37.3 Hz).

Applying spectral decomposition can improve the feasibility of minor fault interpretation. Tuning cubes highlight the amplitude and phase spectrum characteristics in the frequency domain, and provide more abundant geological information of the target area. The common frequency cubes highlight the seismic response of a target at a given frequency, and provide more detailed spatial geological features (Wei and X.D, 2010).

4.4.2 Identifying prospect hydrocarbon zones.

In this study, spectral decomposition is used to identify the prospect hydrocarbon zones of Fimkassar area. The results from spectral decomposition are confirmed by petrophysical analysis performed later in Chapter# 05.

Spectral decomposition performed on three seismic lines that are S96-PW-04, S96-PW-02, G884-FMK-106.

- **Work Flow:**

Compete work flow adopted for spectral decomposition for this study is given below

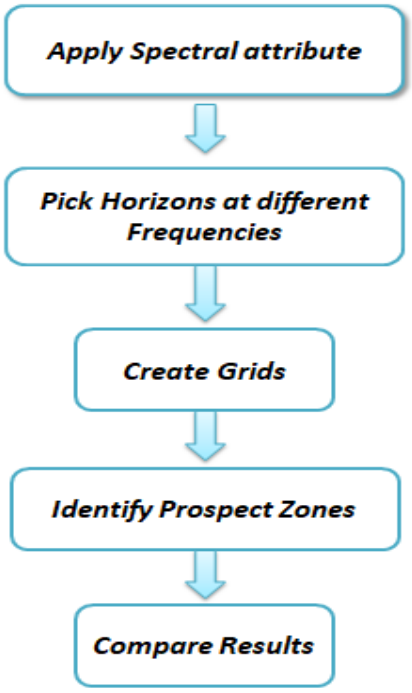

Figure 4.5: Work flow adopted for spectral decomposition for this study.

4.5 Comparison of Grids at Different Frequency Ranges:

Grids made on different formations by selecting different frequencies and then compared and those frequencies are selected which give best results in regard of hydrocarbon accumulation.

4.5.1 Chorgali Grids:

In the first part Chorgali grids are compared at different frequencies. The frequency band of the seismic data is 10-80 Hz (10 Hz, 12.4 Hz, 15.5 Hz, 19.3 Hz, 24.0 Hz, 30 Hz, 37.3 Hz, 46.5 Hz, 58.0 Hz).

In the Figure 4.6, 4.7, 4.8, I explain Chorgali grids at different frequency ranges.

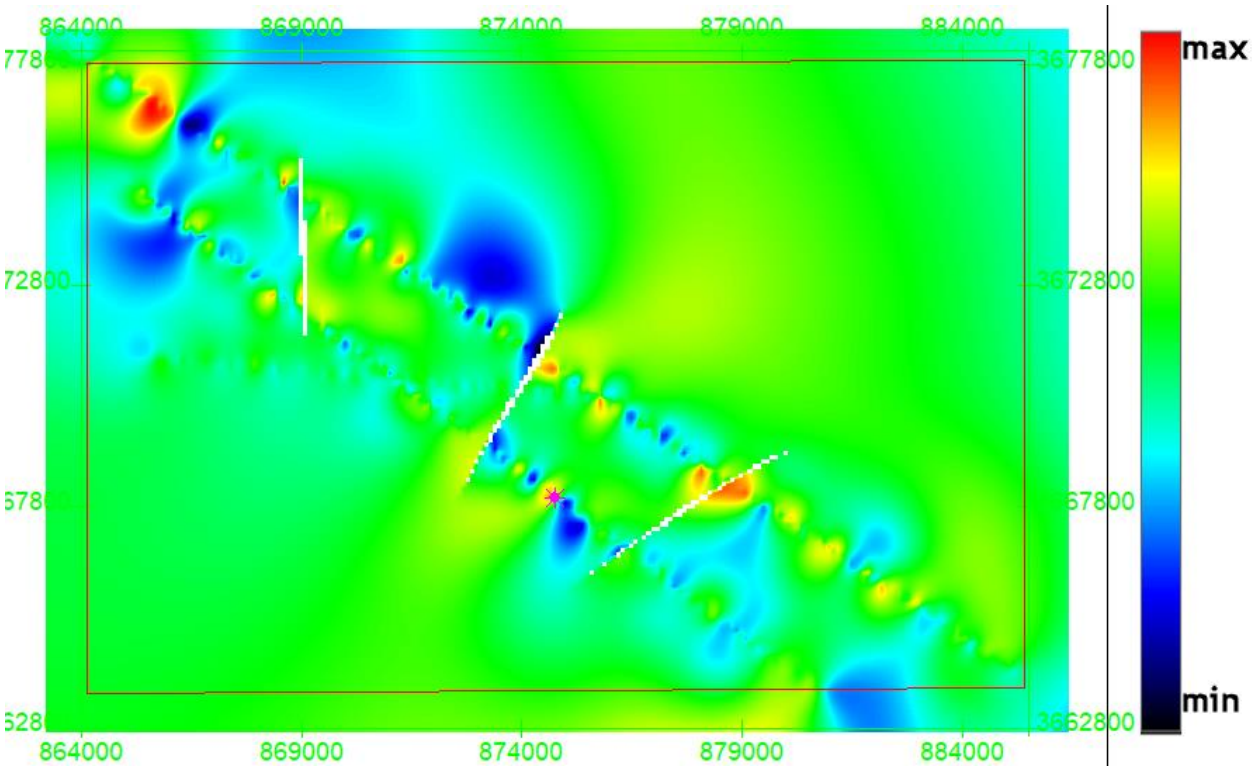

Figure 4.6: Chorgali grid at 15Hz.

In the above Figure, i.e. 4.6 we clearly see that results are not much clear. We must choose that frequency range which give clue about the hydrocarbon accumulation.

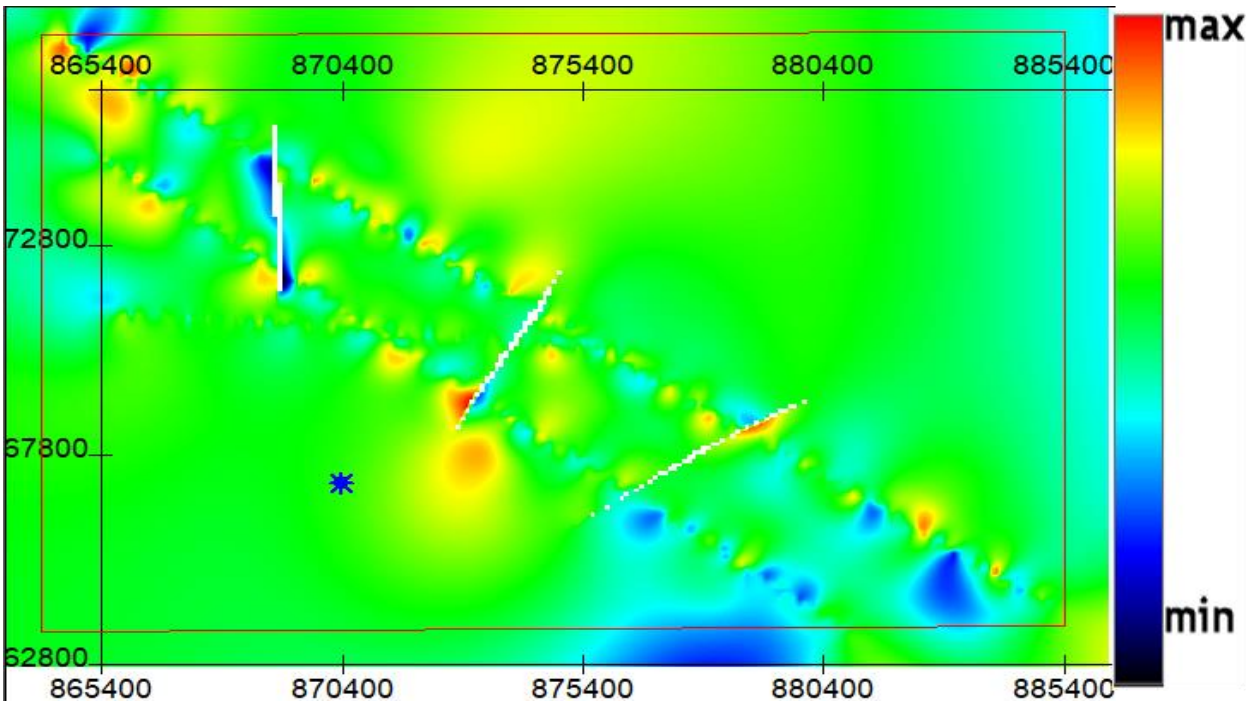

Figure 4.7: Chorgali grid at 30 Hz.

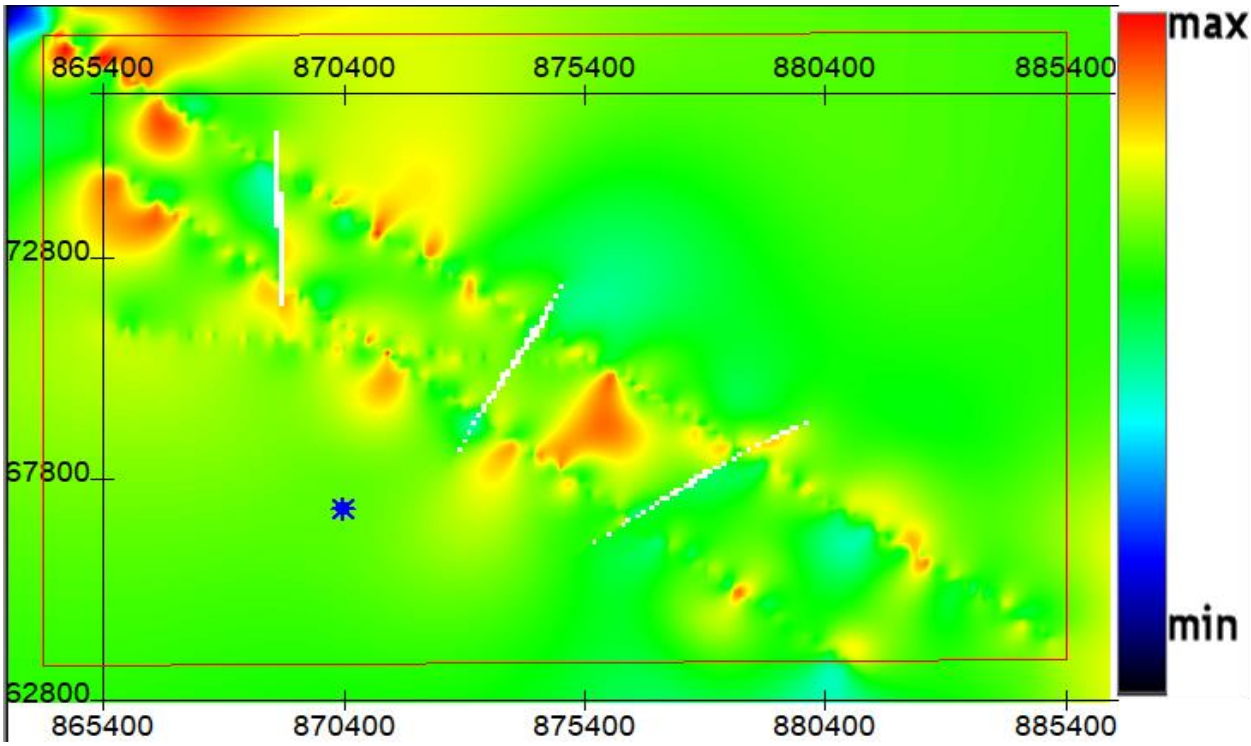

Figure 4.8: Chorgali grid at 37.3 Hz.

4.5.2 Sakesar Grid:

In the second part Sakesar grids are compared at different frequencies. The frequency band of the seismic data is 10-80 Hz (10Hz, 12.4Hz, 15.5Hz, 19.3Hz, 24.0Hz, 30Hz, 37.3Hz, 46.5Hz, 58.0Hz).

In the Figure 4.9, 4.10, 4.11, I explain grids at different frequency range.

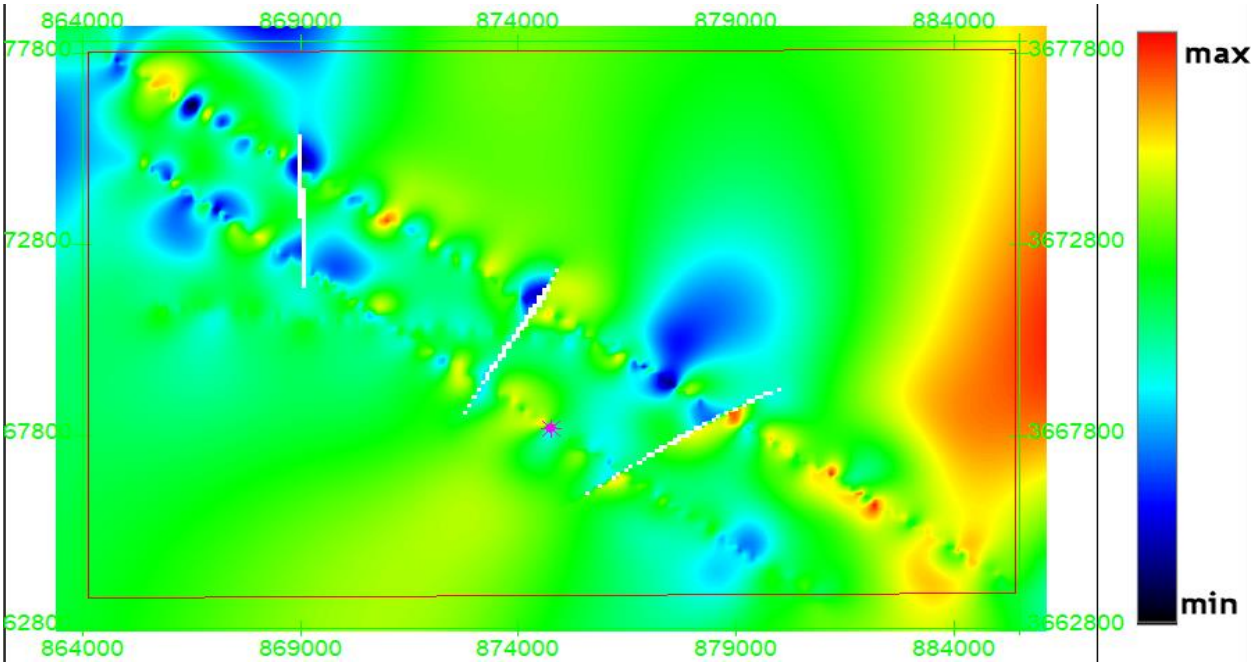

Figure 4.9: Sakesar grid at 15Hz.

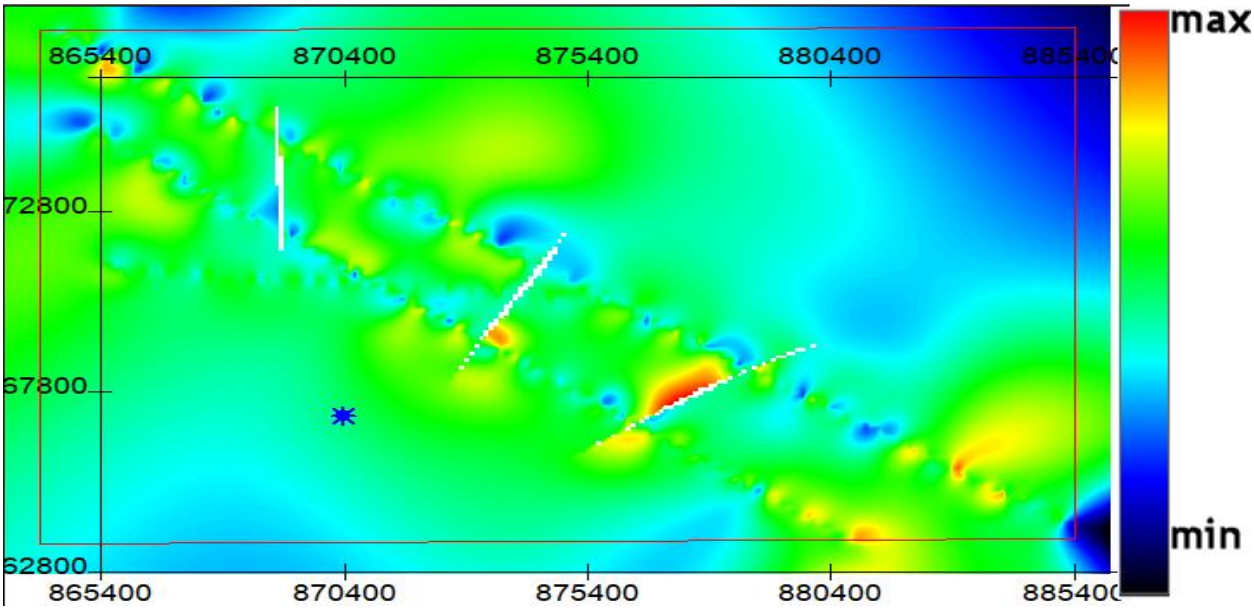

Figure 4.10: Sakesar grid at 30Hz.

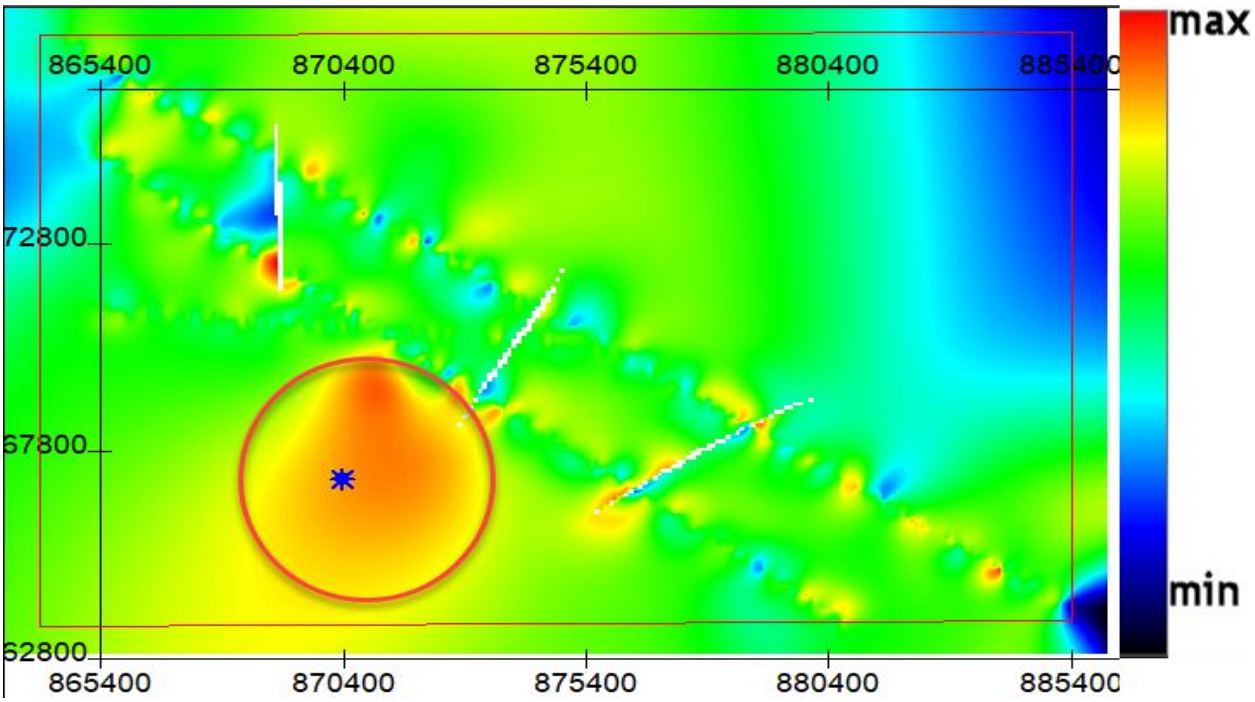

Figure 4.11: Sakesar grid at 37.3Hz.

Figure 4.11 the red circle gives the indication of hydrocarbon, clearly seen from the figure that well Fimkassar-02 lies in the center of the circle so we can say that 37.3 Hz frequency is the best frequency where we get best results. The grid in Figure 4.11 is of Sakesar Formation and these results are confirmed by the petrophysical analysis of Sakesar Formation of well name Fimkassar-02 (Figure 5.5) which gives the results that Sakesar formation is more producing then Chorgali Formation (Ali et al., 2014).

A more detailed analysis of the spectral decomposition shows that 37.3 Hz is the best frequency for imaging prospect hydrocarbon zone in Sakesar Formation.

CHAPTER# 05

PETROPHYSICS

5.1 Introduction:

The general purpose of petrophysical interpretation is to determine the potential hydrocarbon and water bearing zones in a formation by evaluating the raw log data and to estimate the quantities of probable hydrocarbon and water accumulation in those reservoir zones (Ali et al., 2014)

Petrophysical interpretation uses all kind log data, core data to estimate the physical properties such as volume of shale, porosity, water saturation and permeability, which are related to production parameters

5.2 Well Data Used:

By using the well log data of Fimkissar-02 this petrophysical analysis is carried out explained in the Figure 5.1 to determine the potential hydrocarbon.

5.3 Logs Used:

Table 5.1: Logs Used and their Scales.

S/N	Type of Logs	Acronym	Scale Used	Units
1	Caliper Log	CALI	4.0-16.0	Feet
2	Spontaneous Log	SP	-100-100	mV
3	Gamma Ray Log	GR	0-100	API
4	Micro-Spherical Focused Log	MSFL	0.20-4000	Ωm
5	Laterolog Deep	LLD	0.20-4000	Ωm
6	Laterolog Shallow	LLS	0.20-4000	Ωm
7	Sonic Log	DT	140-40	µsec/ft
8	Neutron Log	NPHI	0.45- (-0.15)	PU
9	Density Log	RHOB	1.95-2.95	gm/cm^3

Table 5.2: Logs Used in different Tracks.

Tracks	**Logs**
Track:1	• Caliper log • SP log • GR log
Track:2	• MSFL • LLD • LLS
Track:3	• NPHI • RHOB • DT
Track:4	• VSH
Track:5	• PHID
Track:6	• PHIT
Track:7	• PHIE
Track:8	• SW

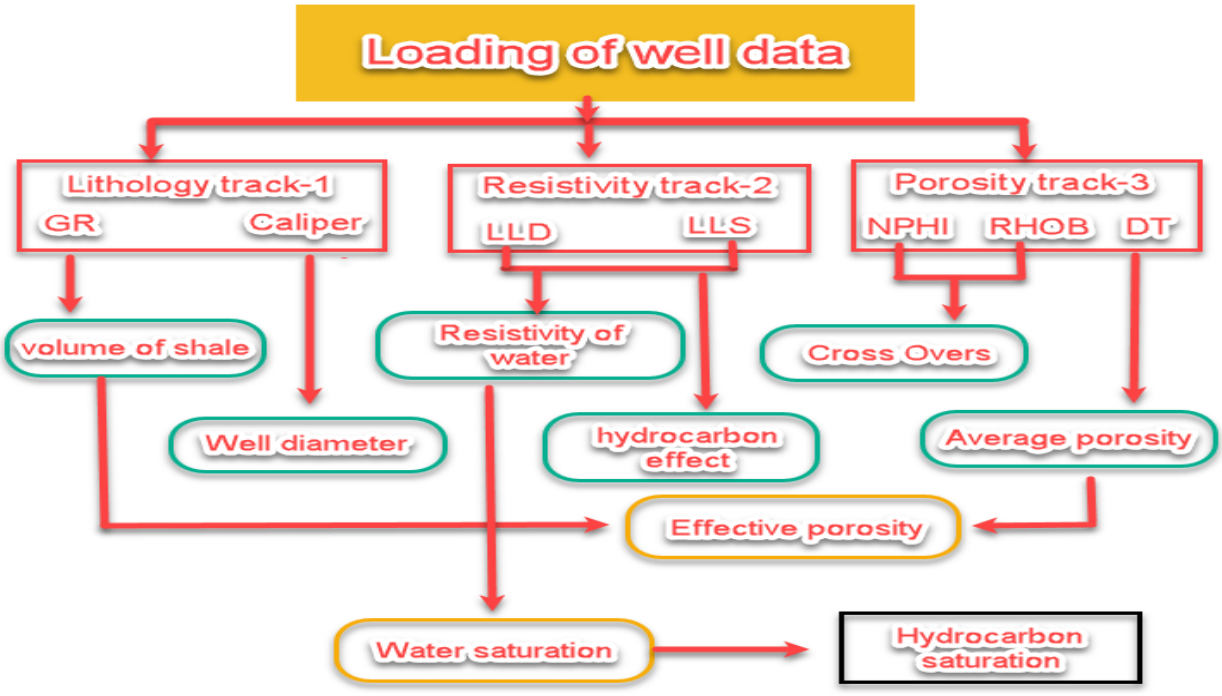

Figure 5.1: Petrophysical analysis work flow.

5.4 Volume of Shale:

Volume of shale can be calculated from different logs like resistivity logs, SP log and gamma ray log. In this study gamma ray log is used to calculate shale volume.

5.4.1 Gamma Ray Log:

The gamma ray log is the passive log because we measure the Formation properties without using any source. It is the measures the Formation radioactivity. The gamma ray emits from the Formation in the form of the electromagnetic energy which are called the photon. When photon collides with the Formation electron they transfer the energy to the Formation electron so the phenomenon of the Compton scattering occurs. Now these emitted Gamma rays reached to the detector of the gamma ray and counted and displayed as count per second which is termed as the Gamma ray (Asquith and Gibson, 2004).

5.4.2 Calculation of Volume of Shale:

The volume of the shale is calculated by using (Asquith and Gibson, 2004) equation given below.

$$\text{IGR}=\frac{GR(log)-GR(min)}{GR(max)-GR(min)}. \qquad 5.1$$

Where,

IGR= Gamma ray index.

GR(max)= Maximum value of Gamma ray reading (Shale).

GR(min)= Minimum value of Gamma ray reading (Clean Sand).

GR(log)= Gamma ray reading of formation.

5.5 Porosity:

Porosity is created due to inter granular spaces, voids formed by dissolution of grains as well as fracturing of rocks. The porosity is expressed either by percentage or in decimals. The primary porosity is developed between the grains at the time of deposition, but due to fracturing and dissolution the pore spaces become void creating secondary porosity. Secondary porosity is mainly observed in limestone. In this work porosity is calculated for different zones of interest by using the following logs, sonic log, neutron log, density log.

5.5.1 Calculation of Porosity from Sonic Log:

- **Sonic Log:**

Sonic log device consists of a transmitter that emit sound waves and a receiver that picks and record the compressional waves as it reaches the receiver. This log is a recording verses depth of time (t) which is required by a compressional wave to go across 1 feet of formation, called interval transient time Δt, while it is the reciprocal of the velocity of sound wave. This time (Δt) is depended upon lithology and porosity of the formation (Asquith and Gibson, 2004).

The mathematical relation used for the calculation of porosity from sonic log is given below.

$$\Phi s = \frac{\Delta t(log) - \Delta t(mat)}{\Delta t(fl) - \Delta t(mat)}. \qquad 5.2$$

Where,

Φs= Sonic Porosity.

Δt(log)= Log response.

Δt(mat)= Transit time in matrix.

Δt(fl)= Transit time in fluid.

5.5.2 Calculation of Porosity from Density Log:

- **Density Log:**

Gamma rays collide with electrons in formation and scattered gamma rays received at detector and counted as indicator of formation density. An increase in counting rate causes a decrease in bulk density of formation and vice versa. (Tittman and Wahal, 1965).

The mathematical relation used for the calculation of porosity from density log is given below.

$$\Phi_D = \frac{\rho m - \rho b}{\rho m - \rho f}. \qquad 5.3$$

Where,

ρm= Matrix density.

ρb= Bulk density.

ρf= Fluid density.

5.5.3 Calculation of Average Porosity:

Average porosity is the sum of all the porosities calculated by different logs divided by number of logs used for calculating the porosity. The relation for calculating the average porosity is given below.

$$\Phi_{avg} = \frac{\Phi s + \Phi d}{2}. \qquad 5.4$$

Where,

Φ_{avg}=Average porosity

Φ_s=Sonic porosity.

Φ_d=Density porosity.

5.5.4 Calculation of Total Porosity:

Total porosity has been calculated by the help of following formula.

$$\Phi_T = 2(\Phi s + \Phi d). \qquad 5.5$$

Where,

Φ_T=Total porosity.

Φ_s=Sonic porosity.

Φ_d=Density porosity.

5.5.5 Calculation of Effective Porosity:

Effective porosity is calculated by following formula

$$\Phi_s = \Phi_{avg} * (1\text{-Volume of shale}). \qquad 5.6$$

5.6 Calculation of Water Saturation (Sw):

To calculate saturation of water in the formation, a mathematical equation was developed by Archie given in equation (5.7) given below. At 0.5 cut off is used to separate the water and hydrocarbon.

$$S_w = \sqrt[n]{\frac{F \times R_w}{R_t}}. \qquad 5.7$$

Where,

Sw= Water saturation.

F=Formation Factor($F = \frac{a}{\phi m}$).

Rt= True resistivity.

n= Saturation component value ranges from 1.8 to 2.5.

a= Constant value (with a constant value 1).

Ø= Effective porosity.

m= Cementation factor (with a constant value 2).

5.6.1 Calculation of Resistivity of Water (R_w):

Formation water resistivity (R_w) was calculated with the help of certain parameters like bottom hole temperature, surface temperature, water salinity in (ppm)and static spontaneous potential. For the calculation of resistivity of water following steps are fallowed

1. Read the SP value at the depth of maximum deflection, which gives SSP and is calculated by using the equation given below

$$\mathbf{SSP} = SP_{clean} - SP_{shale}$$

Where,

SSP = Static Spontaneous Potential.

SP_{clean}= Spontaneous potential for sand.

SP_{shale}= Spontaneous potential for shale.

Values for the well Fimkassar-02 used are given in the table given below

Table 5.3: Value of SSP, SP_{clean}, SP_{shale} for the well Fimkassar-02.

Fimkassar-02			
S/N	**SSP**	**SP_{clean}**	**SP_{shale}**
1	-60 mv	0	60

2. Calculate the formation temperature (FT) from relation given in equation below at the depth of the SP value. Use Gen-6, (Schlumberger chart) given in appendix-1, with total depth and maximum temperature from the log header.

$$FT = \left[\frac{(BHT-ST)}{TD} \times FD\right]. \quad 5.8$$

Where,

FT = Formation temperature.

BHT = Borehole temperature.

FD = Formation depth (from surface to Fm).

ST = Surface temperature.

TD = Total depth (from surface to end).

3. Resistivity of mud filtrate (R_{mf1}) at surface temperature (ST= 26℃) is calculated using Gen-6 (Schlumberger chart) given in appendix-1, and it is 0.479 Ωm for well Fimkassar-02.

4. Calculate the resistivity of mud filtrate at zone of interest (FT) and it is calculated by equation given below

$$R_{mf2} = \frac{(ST+6.77)\times R_{mf1}}{(FT+6.77)}. \quad 5.9$$

Where,

R_{mf1}= Resistivity of mud filtrates at surface temperature (from well header).

ST= Surface temperature.

FT= Formation temperature.

R_{mf2}= Resistivity of mud filtrates at formation temperature. (R_{mf2}= 0.196 Ωm for Fimkassar-02).

5. Calculate Resistivity of mud filtrate equivalent (R_{mfeq}) at formation temperature, this is performed by considering the following, two conditions

- If R_{mf2} is greater than 0.1 Ωm then correct it to formation temperature using the following relationship given in equation given below.

$$R_{mfeq} = 0.85 \times R_{mf2}. \qquad 5.10$$

- If R_{mf2} is less than 0.1 (Ωm) then use chart SP-2 (Schlumberger Chart) given in appendix-2 to derive a value of R_{mfeq} at formation temperature.

5.6.2 Calculation of Resistivity of water Equivalent (R_{weq}) and R_w:

SSP is difference of maximum and minimum value of SP log. SSP is -60 mv and is plotted on Gen-6 (Schlumberger chart)

- **For True Rw:**

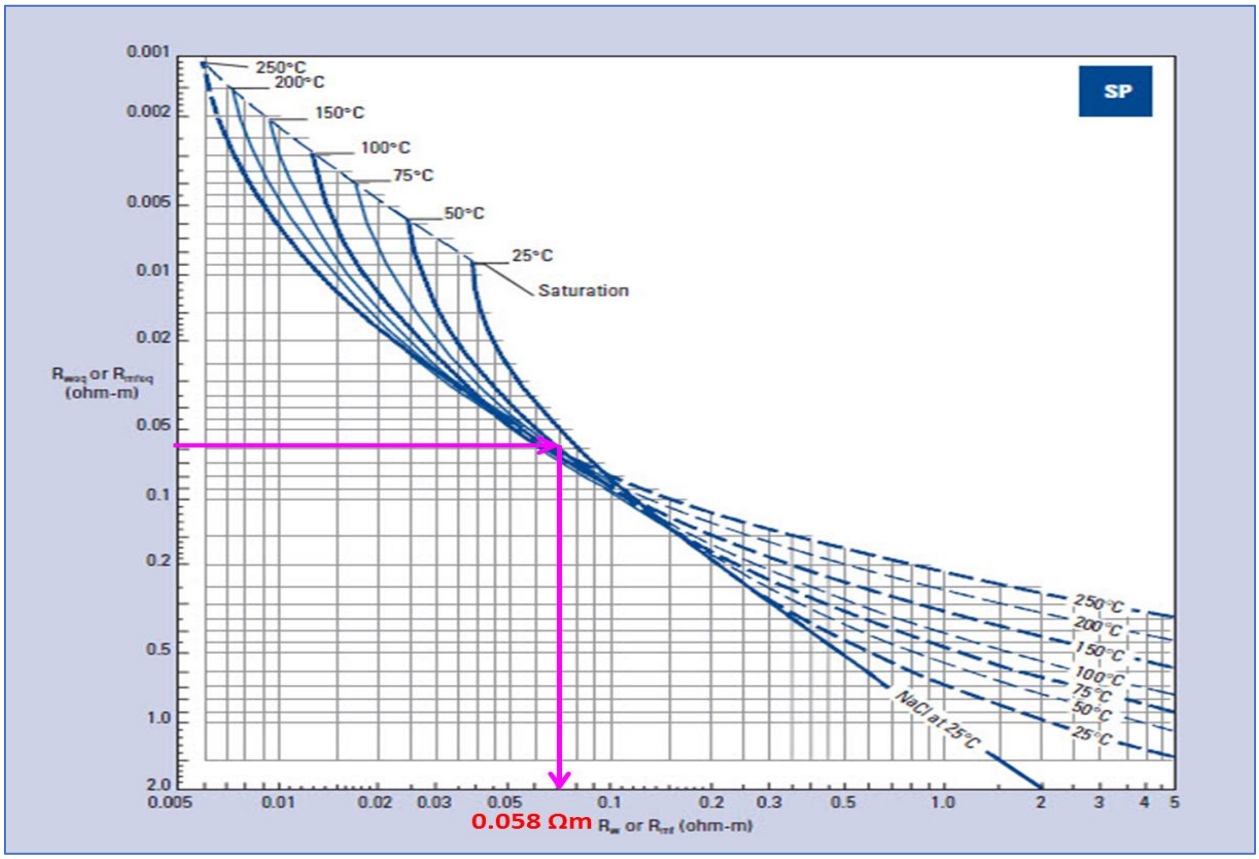

Figure 5.2 Determination of Rw from SP chart (Schlumberger, 1989).

5.7 Well Log Interpretation of Fimkassar-02

Petrophysical analysis of Fimkassar-02 is interpreted based on the behavior of different log curves using SMT Kingdom (8.8). As a first indicator of lithology, GR log is very useful for the indication of shale. For the higher values of GR, higher will be the percentage of shale. Where there is low value of the GR shows less shale So, due to this reason, clean zone or shale free zone is defined easily so its mean that may be hydrocarbon bearing zone is available. Resistivity logs are used to give the volume of oil/gas in a reservoir, or, in petrophysical terms, to define the water saturation (Sw). When Sw is not 100%, then its shows hydrocarbons are present there. Higher the response of resistivity logs usually determines the presence of hydrocarbons or fresh water. Density mainly varies from 2.55 to 2.99 g/cm^3. But somewhere at the reservoir level, very high density corresponding to low resistivity is noted.

5.7.1 Petrophysical Interpretation of Chorgali Formation:

Petrophysical interpretation is carried out for Chorgali Formation starts at a depth of 2902m to 2946m with a total thickness of 44m.

- **For a whole depth of Chorgali Formation:**

Table 5.4: For whole depth of Chorgali Formation.

Average Volume of shale in %age	34%
Average density porosity in %age	9%
Average porosity in %age	10%
Average effective porosity in %age	5%
Average water saturation in %age	58%
Average hydrocarbon saturation in %age	42%

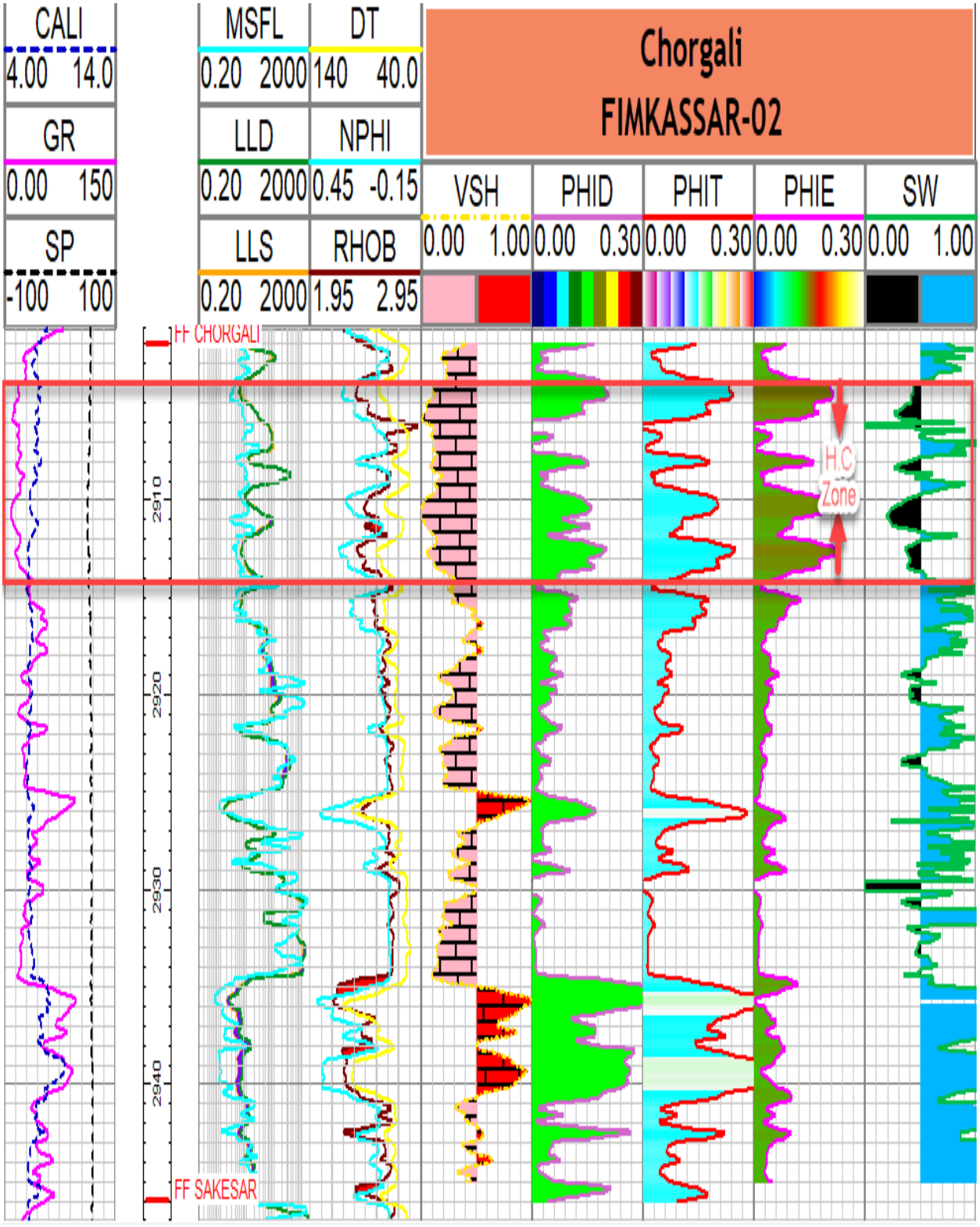

Figure 5.3: Petrophysical interpretation of the well Fimkassar-02 with possible hydrocarbon zone.

- **For zone of interest of Chorgali Formation:**

Table 5.5: For interested zone in Chorgali Formation.

Average Volume of shale in %age	19%
Average density porosity in %age	8%
Average porosity in %age	11%
Average effective porosity in %age	9%
Average water saturation in %age	51%
Average hydrocarbon saturation in %age	49%

5.7.2 Petrophysical Interpretation of Sakesar Formation:

Petrophysical interpretation is carried out for Sakesar formation starts at a depth of 2947m to 3069m with a total thickness of 122m.

- **For a whole depth of Sakesar Formation:**

Table 5.6: For whole depth of Sakesar Formation.

Average Volume of shale in %age	37%
Average density porosity in %age	5%
Average porosity in %age	4%
Average effective porosity in %age	2%
Average water saturation in %age	59%
Average hydrocarbon saturation in %age	41%

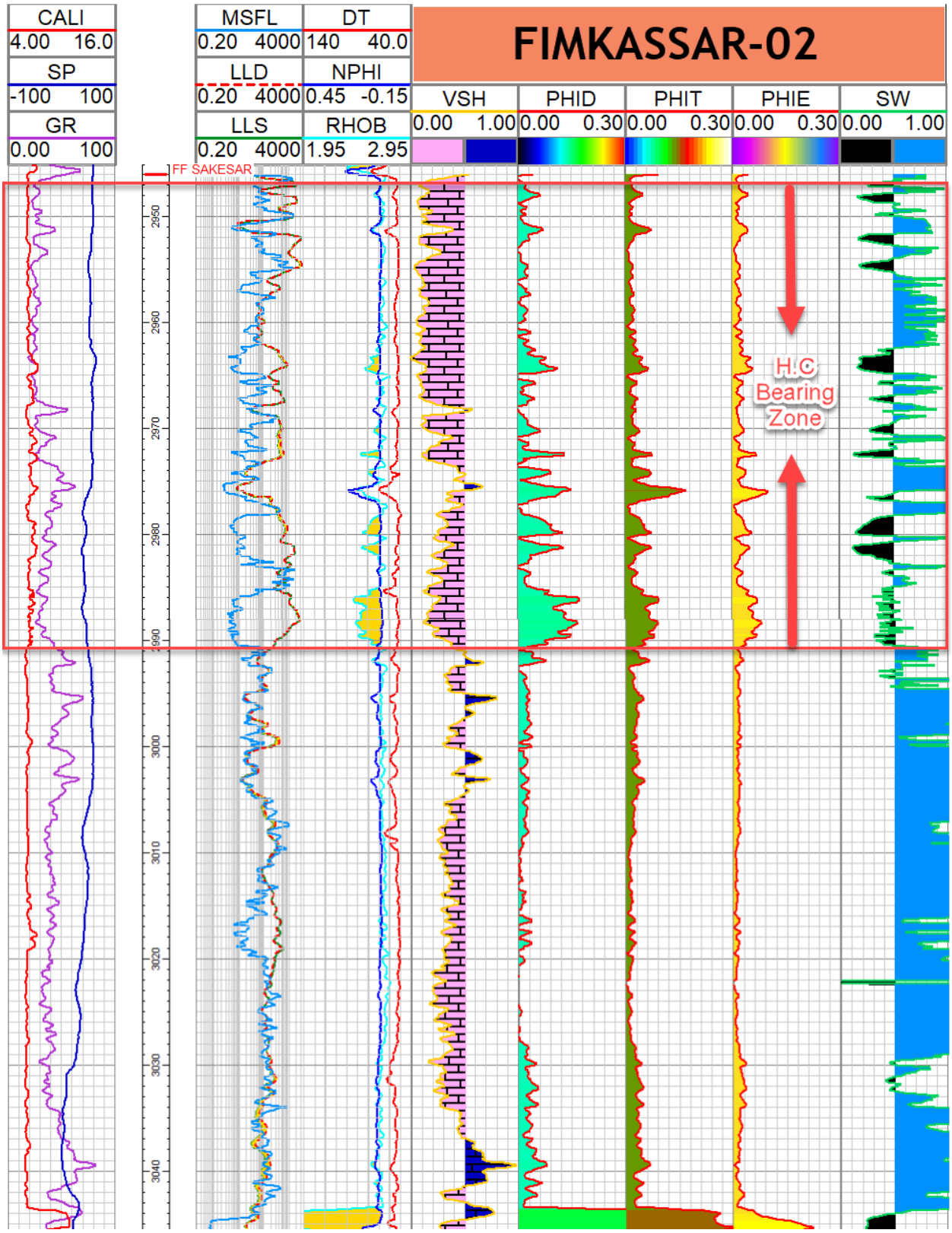

Figure 5.4: Petrophysical interpretation of the well Fimkassar-02 with possible hydrocarbon zone.

- **For zone of interest of Sakesar formation:**

Table 5.7: For interested zone of Sakesar Formation.

Average Volume of shale in %age	21%
Average density porosity in %age	4%
Average porosity in %age	3%
Average effective porosity in %age	4%
Average water saturation in %age	45%
Average hydrocarbon saturation in %age	55%

Conclusions:

- Time and Depth contour maps of Chorgali and Sakesar Formation help us to confirm the presence of anticlinal and snake head structure in the given area. Surface contour map of Chorgali and Sakesar Formation gives the real shape of sub-surface structure, which is anticlinal. This anticlinal and snake head structure acts as a trap in the area, which is best for hydrocarbon accumulation. This shows that the study area is dominated by compressional tectonic forces.
- The pseudo-synthetic trace is generated via well log confirms the marking of right seismic sections.
- The seismic attribute analysis of given 2D data confirms the interpretation also for the detection of hydrocarbon, rate of sedimentation and its preservation at some locations but not give any reliable location to identify hydrocarbons.
- By Spectral decomposition we can estimate the possible zones for hydrocarbon accumulation by making grid of Chorgali and Sakesar Formation at different frequencies. These results from spectral decomposition are confirmed by petrophysical analysis.
- Petrophysical analysis of the reservoir of the well Fimkassar-02, shows fine hydrocarbon potential and its concluded results show that Sakesar formation is more hydrocarbon bearing than the Chorgali.

References:

- Aamir, M., & Siddiqui, M. M. (2006). Interpretation and visualization of thrust sheets in a triangle zone in eastern Potwar, Pakistan. *The Leading Edge*, *25*(1), 24-37.
- Ahmad, M., Tasneem, M. A., Rafiq, M., Khan, I. H., Farooq, M., & Sajjad, M. I. (2003). Interwell tracing by environmental isotopes at Fimkassar Oilfield, Pakistan. *Applied radiation and isotopes*, *58*(5), 611-619.
- Ali, A., Kashif, M., Hussain, M., Siddique, J., Aslam, I., & Ahmed, Z. (2015). An integrated analysis of petrophysics, cross-plots and Gassmann fluid substitution for characterization of Fimkassar area, Pakistan: A case study. *Arabian Journal for Science and Engineering*, *40*(1), 181-193.
- Ali, A., Kashif, M., Hussain, M., Siddique, J., Aslam, I., & Ahmed, Z. (2015). An integrated analysis of petrophysics, cross-plots and Gassmann fluid substitution for characterization of Fimkassar area, Pakistan: A case study. *Arabian Journal for Science and Engineering*, *40*(1), 181-193.
- Asquith, G. B., Krygowski, D., & Gibson, C. R. (2004). *Basic well log analysis*(Vol. 16). Tulsa: American association of petroleum geologists.
- Badley, M. E. (1985). Practical seismic interpretation.
- Banks, C. J., & Warburton, J. (1986). 'Passive-roof'duplex geometry in the frontal structures of the Kirthar and Sulaiman mountain belts, Pakistan. *Journal of Structural Geology*, *8*(3-4), 229-237.
- Bender, F., & Raza, H. A. (1995). Geology of Pakistan.
- Castagna, J. P., Sun, S., & Siegfried, R. W. (2003). Instantaneous spectral analysis: Detection of low-frequency shadows associated with hydrocarbons. *The leading edge*, *22*(2), 120-127.
- Coffeen, J. A. (1986). Seismic exploration fundamentals.
- Davies, L. M., & Pinfold, E. S. (1937). The Eocene beds of the Punjab Salt Range; Appendix: Correlation of the Salt Range beds with Eocene beds of Tibet. *India, Geol. Survey, Mem., Pal. Indica, new ser*, *24*(1), 68-71.
- Gee, E. R., & Gee, D. G. (1989). Overview of the geology and structure of the Salt Range, with observations on related areas of northern Pakistan. *Geological Society of America Special Papers*, *232*, 95-112.
- Handwerger, D. A., Cooper, A. K., O'Brien, P. E., Williams, T., Barr, S. R., Dunbar, R. B., ... & Jarrard, R. D. (2004). Synthetic seismograms linking ODP sites to seismic profiles, continental rise and shelf of Prydz Bay, Antarctica. *Cooper, AK, O'Brien, PE, and Richter, C., et al., Proceedings of the Ocean Drilling Program, Scientific Results*, *188*, 1-28.
- Kazmi, A. H., & Jan, M. Q. (1997). *Geology and tectonics of Pakistan*. Graphic publishers.
- Khan, M. A., Ahmed, R., Raza, H. A., & Kemal, A. (1986). Geology of petroleum in Kohat-Potwar depression, Pakistan. *AAPG Bulletin*, *70*(4), 396-414.

- Khonde, K., & Rastogi, R. (2013, November). Recent developments in spectral decomposition of seismic data (techniques and applications): a review. In *10th Biennial International Conference & Exposition* (pp. 28-34).
- Marfurt, K. J., & Kirlin, R. L. (2001). Narrow-band spectral analysis and thin-bed tuning. *Geophysics*, *66*(4), 1274-1283.
- Oyeyemi, K. D., & Aizebeokhai, A. P. (2015). Seismic attributes analysis for reservoir characterization; offshore Niger Delta. *Petroleum and coal*, *57*(6), 619-628.
- Partyka, G., Gridley, J., & Lopez, J. (1999). Interpretational applications of spectral decomposition in reservoir characterization. *The Leading Edge*, *18*(3), 353-360.
- Partyka, G., Gridley, J., & Lopez, J. (1999). Interpretational applications of spectral decomposition in reservoir characterization. *The Leading Edge*, *18*(3), 353-360.
- Shami, B. A., & Baig, M. S. (2002, November). Geomodeling for enhancement of hydrocarbon potential of Joya Mair Field (Potwar) Pakistan. In PAPG-SPE Annual Technical Conference, Islamabad (pp. 124-145).
- Slatt, R. M. (2006). *Stratigraphic reservoir characterization for petroleum geologists, geophysicists, and engineers* (Vol. 61). Elsevier.
- Taner, M. T. (2001). Seismic attributes. *CSEG recorder*, *26*(7), 48-56.
- Taner, M. T., Schuelke, J. S., O'Doherty, R., & Baysal, E. (1994). Seismic attributes revisited. In *SEG Technical Program Expanded Abstracts 1994* (pp. 1104-1106). Society of Exploration Geophysicists.
- Tittman, J., & Wahl, J. S. (1965). The physical foundations of formation density logging (gamma-gamma). *Geophysics*, *30*(2), 284-294.
- Wei, X. D. (2010, June). Interpretational Applications of Spectral Decomposition in Identifying Minor Faults. In *72nd EAGE Conference and Exhibition incorporating SPE EUROPEC 2010*.